Radiation Effects on Silica-Based Optical Fibers: Recent Advances and Future Challenges

S. Girard, *Senior Member, IEEE*, J. Kuhnhenn, A. Gusarov, B. Brichard, M. Van Uffelen, *Senior Member, IEEE*, Y. Ouerdane, A. Boukenter, and C. Marcandella

***Abstract*—In this review paper, we present radiation effects on silica-based optical fibers. We first describe the mechanisms inducing microscopic and macroscopic changes under irradiation: radiation-induced attenuation, radiation-induced emission and compaction. We then discuss the influence of various parameters related to the optical fiber, to the harsh environments and to the fiber-based applications on the amplitudes and kinetics of these changes. Then, we focus on advances obtained over the last years. We summarize the main results regarding the fiber vulnerability and hardening to radiative constraints associated with several facilities such as Megajoule class lasers, ITER, LHC, nuclear power plants or with space applications. Based on the experience gained during these projects, we suggest some of the challenges that will have to be overcome in the near future to allow a deeper integration of fibers and fiber-based sensors in radiative environments.**

***Index Terms*—Absorption, color centers, fiber sensors, ITER, LHC, LMJ, luminescence, optical fibers, radiation effects, radiation induced attenuation, silica, space.**

I. Introduction

THE vulnerability of numerous fiber-based applications has been or is currently being studied to evaluate their performances and lifetimes when exposed to radiative constraints associated to natural or artificial environments. Depending on the targeted applications, various harsh environments have to be considered in terms of particles, dose and dose rate. In Fig. 1, we review some of these environments for which the radiation sensitivity of optical fibers has been recently investigated.

Manuscript received July 27, 2012; revised December 05, 2012; accepted December 11, 2012.

S. Girard, Y. Ouerdane, and A. Boukenter are with Université de Saint-Etienne, Laboratoire Hubert Curien, UMR CNRS 5516, Saint-Etienne, France (e-mail: sylvain.girard@univ-st-etienne.fr; ouerdane@univ-st-etienne.fr; aziz.boukenter@univ-st-etienne.fr).

J. Kuhnhenn is with Fraunhofer-Institut für Naturwissenschaftlich-Technische Trendanalysen, Appelsgarten 2, D-53879 Euskirchen, Germany (e-mail: jochen.kuhnhenn@int.fraunhofer.de)

A. Gusarov is with the SCK CEN Belgian Nuclear Research Center, Boeretang 200, 2400 Mol, Belgium (e-mail: agusarov@sckcen.be).

B. Brichard and M. Van Uffelen are with F4E, 08019 Barcelona, Spain (e-mail: marco.vanuffelen@f4e.europa.eu; benoit.brichard@f4e.europa.eu).

C. Marcandella is with CEA, DAM, DIF, F91297 Arpajon, France (e-mail: claude.marcandella@cea.fr).

Color versions of one or more of the figures in this paper are available online at http://ieeexplore.ieee.org.

Digital Object Identifier 10.1109/TNS.2012.2235464

For data transmission in such environments, optical fibers present several advantages compared to copper cables. Contrary to coaxial cables, they can be considered as immune to most of the electromagnetic perturbations associated with these projects, such as the ones associated with megajoule class laser facilities (Laser Megajoule (LMJ), National Ignition facility (NIF)) devoted to the study of fusion by inertial confinement [1]. Furthermore, optical waveguides present a low attenuation (typically 0.2 dB/km at 1550 nm), a high bandwidth and a multiplexing capability that allow transmission of the large amounts of data acquired at high energy physics facilities like the Large Hadron Collider (LHC) [2]. The low weight and volume associated with these transmission links are key advantages for their use in a spacecraft [3], [4] or to develop plasma diagnostics for fusion facilities, such as the International Thermonuclear Experimental Reactor (ITER), LMJ or NIF [5], [6]. Optical fibers can also be functionalized to serve as distributed or discrete sensors for various parameters such as temperature, strain, pressure or radiations for civil nuclear applications or nuclear waste storage [7], [8].

Despite their many advantages, radiation still degrades the optical fiber properties, through three different mechanisms: radiation-induced attenuation (RIA), radiation induced emission (RIE) and compaction. The amplitudes and kinetics of these changes strongly depend on the tested fiber and application requirements. Today, the fiber response remains too complex to be fully predictable. Radiation testing remains necessary, first to evaluate the vulnerability of fibers to one specific environment for one given application and second, to investigate different radiation hardening strategies (hardening by design or hardening by system). In the past, several review papers were proposed on this thematic by different research groups [10]–[12]. In this paper, we mainly focus our discussion on experimental results and knowledge acquired during the last decade. The structure of the paper is the following: we briefly introduce the basic mechanisms occurring in the pure or doped amorphous silica glass constituting the fiber core and cladding and the macroscopic changes observed in these devices under irradiation. Then, we review the different intrinsic and extrinsic parameters that are known to influence their radiation sensitivities, giving some examples of fiber responses and some overview about the radiation induced mechanisms and related point defects. In addition, we present summaries of the most important results acquired during the past years through radiation effects studies on fibers for today or future facilities such as megajoule class lasers, ITER, LHC, nuclear industry or for space applications.

Finally, based on this work, we discuss future challenges for our community.

II. Properties of Silica-Based Glasses and Radiation Effects at the Microscopic and Macroscopic Scale

Understanding radiation effects on silica-based optical fibers implies identifying and characterizing the changes occurring at different scales in pure or doped amorphous silica (a-SiO_2). If the fiber vulnerability for a given application is mainly linked to the degradation of one of its macroscopic properties, the knowledge of radiation-induced mechanisms at atomic scale remains mandatory to understand the origin of these degradations and to be able to propose hardening techniques. Such understanding necessitates considering the interactions between neutral (*photons, neutrons*) or charged particles (*electrons, protons*) with a-SiO_2 and their consequences at different scales, from atomic to device level. In this part, we first briefly present a-SiO_2 glass properties and radiation-induced effects at atomic scale by introducing the concept of radiation-induced point defects. Second, we describe typical fiber structures and discuss how the structure chosen for the fiber design can affect its radiation response.

A. Description of a-SiO_2,

The a-SiO_2 building unit is the SiO_4 tetrahedron, like in the quartz crystalline structure. In this unit, the central silicon (Si) atom is bonded to four oxygen (O) atoms which occupy the corners of the tetrahedron [see Fig. 2(a)] [13]. The perfect silica structure can be viewed as a continuous random network of these units joined at the corners. The amorphous state can be described by means of a randomness degree, lack of periodicity and breaking of the long range order, as illustrated in Fig. 2(a). As opposed to the quartz crystal, the parameters defining the glass, such as Si-O-Si angles or Si-O bond lengths are not well-defined but are characterized by a continuous distribution around a mean value [14]. Ideal amorphous silica is usually described through the Continuous Random Theory (CRN) [15]. The tetrahedral units correspond to the short range. The second (medium) range extends to the interconnections between adjacent units and the third (long) range refers to the network topology and rings statistics. Specific CRN models have been deduced from X-ray and neutron diffraction experiments, a review on these amorphography studies is given in [16].

In bulk and optical fibers, the nature of glass is more complex due to the presence of intrinsic or extrinsic point defects that are induced during the glass elaboration or under specific treatments [17]. Defect structures are related to under- or over-coordinated atoms, substitutional or interstitial impurities such as Cl or H [see Fig. 2(b)], or bonds between similar atoms (eg. Si-Si or Si-O-O-Si). These defects are associated with absorption bands within the silica bandgap that decrease the glass or fiber transparency. They can either be created during the manufacturing process, by conversion of pre-existing centers under irradiation or directly from "perfect" sites by radiations. A detailed review of these processes can be found in [18].

B. Radiation-Matter Interactions

Two main radiation-matter interactions are involved in defect creation: the knock-on and ionization processes. Direct atomic displacements, also known as knock-on damages, can occur in silica if the incoming particle transfers a sufficient amount of energy to the glass matrix. The displacement threshold energy is of about 10 eV for O and 18 eV for Si [19]. Concerning ionization processes and associated radiolytic processes, electrons from the valence band can be transferred to the conduction band with a certain kinetic energy, which depends on the energy transferred by the incoming particle. Concurrently, a hole is generated in the valence band. The created electron-hole pairs can recombine either radiatively (luminescence) or non-radiatively. In the latter case, the energy is dissipated through the creation of phonons or by secondary radiolytic processes which could lead to the generation of point defects. Mobile charges can also be trapped on pre-existing or radiation-induced sites. External

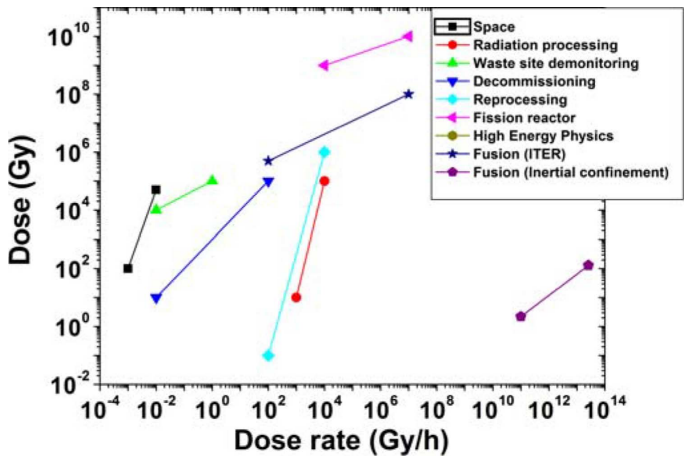

Fig. 1. Typical dose and dose rate ranges associated with various projects and natural radiative environments where the integration of optical fibers is considered. Adapted from [9].

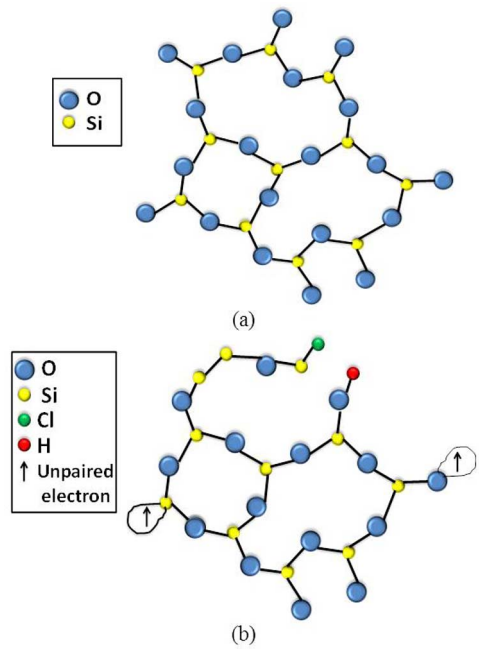

Fig. 2. (a) Ideal pure-silica glass structure (b) Defective pure-silica glass structure.

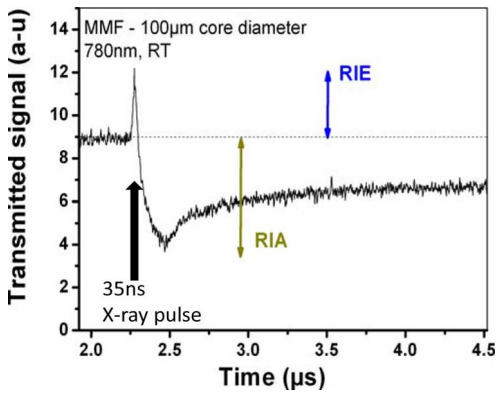

Fig. 3. Radiation-induced changes in the transmission of a multimode optical fiber at 780 nm before, during and after a 35 ns irradiation pulse of 1 MeV X-rays.

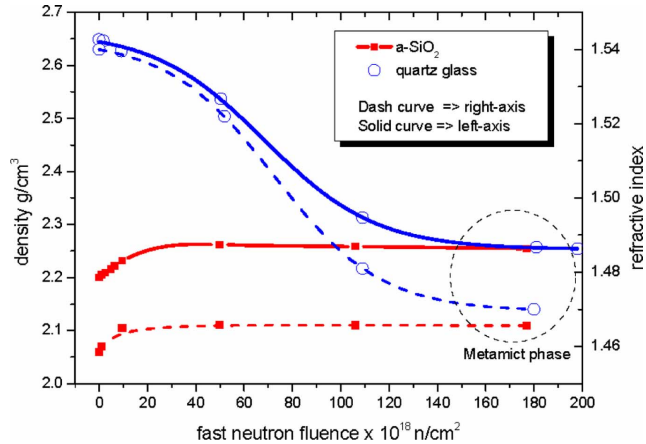

Fig. 4. Density change and corresponding refractive index change induced by neutrons in quartz and amorphous bulk silica (adapted from [20]).

actions, such as photobleaching or thermal treatments, are then required to release the carriers from these traps.

C. Macroscopic Changes Induced by Radiation in Silica-Based Glasses

Three macroscopic effects can be observed in silica-based glasses under irradiation: Radiation Induced Attenuation (RIA), Radiation Induced Emission (RIE) and change in refractive index.

Radiation-Induced Attenuation (RIA) corresponds to an increase in the glass linear attenuation through an increase of the linear absorption due to radiation-induced defects. This is a wavelength-dependent and time-dependent effect.

Radiation-Induced Emission (RIE) corresponds to light emission within the samples under irradiation. It can be luminescence from pre-existing or radiation induced point defects that are excited by the incoming particles (Radiation Induced Luminescence, RIL) or Cerenkov emission. Fig. 3 illustrates the changes induced by a 1 MeV X-ray radiation pulse of 35 ns on the transmission efficiency of a multimode optical fiber at 780 nm.

During the irradiation pulse, at least two mechanisms are in competition: a strong RIA phenomenon and a strong RIE phenomenon—which, for this fiber, mask the RIA (spectral analysis reveals that this RIE is mainly explained by Cerenkov radiation). After the end of the pulse, RIA dominates and the fiber transmission is strongly decreased. The fiber transmission partially recovers during and after the irradiation through thermal bleaching of the radiation-induced point defects at room temperature. At longer times after irradiation, only the point defects which are stable at the experiment temperature contribute to the RIA.

A change in Refractive Index (RI) can stem from density changes or from RIA. The RI change is related to a density change via the Lorentz-Lorenz formula, while the link with the induced absorption effect is described via the Kramers-Krönig relations. In theory, the density effect is also included in the Kramers-Krönig relations but in practice it is more convenient to separate the color centers contribution, responsible for the RIA, and describe the remaining changes as density effects. Compaction or swelling leading to glass density modifications depend on the silica type (crystalline or amorphous). This effect was first observed by Primak [20] in bulk silica irradiated with fast neutrons. He found a density and refractive index increase of 3% (Fig. 4) when amorphous silica was irradiated at a fast neutron fluence larger than 10^{19} $\mathrm{n/cm^2}$, while silica in its α-quartz form exhibits a density decrease of more than 10%. Remarkably, neutron irradiation transforms both silica amorphous and crystal phases into a new common topological structure referred to as the metamict phase [21]. These changes in refractive index affect the optical properties of the fibers, creating additional guiding losses when a fiber is exposed to very high doses.

Among these different phenomena, the RIA is usually the main limiting factor for the integration of optical fibers in radiative environments. RIE also has to be considered, especially when RIA-tolerant optical fibers are used. The amplitudes of these macroscopic changes strongly depend on the characteristics of the tested fibers, on the radiative environments and on the application parameters. The influence of these different parameters on the fiber behavior will be detailed in the next part of this paper.

III. Influence of the Fiber Structure on its Radiation Response

In this section, we discuss differences observed in the radiation responses of two classes of optical fibers often considered for telecommunications or sensing in harsh environments: conventional optical fibers and microstructured optical fibers. The case of rare-earth optical fibers and polarization maintaining optical fibers will be discussed in Section VIII-D. In this review, plastic optical fibers are not considered since only a few studies have been devoted to the radiation response of this particular type of waveguide which seems to be very sensitive to radiation [22], [23].

A. Response of Conventional Passive Optical Fibers

Different classes of commercial-off-the-shelf (COTS) multimode (MM) or single-mode (SM) optical fibers exist. Testing

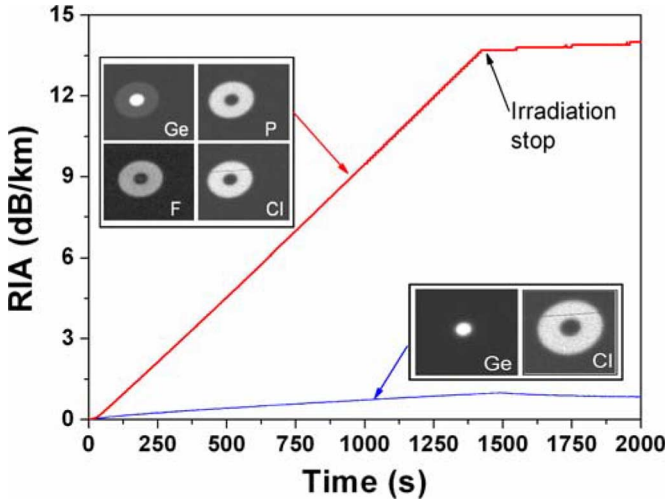

Fig. 5. Radiation induced attenuation (RIA) measured at 1550 nm during and after 0.8 MeV neutron irradiation (flux of 3.5×10^{12} n $\mathrm{cm}^{-2}.\mathrm{s}^{-1}$) for two COTS optical fibers (attenuation of 0.2 dB/km before irradiation) with identical optical properties before irradiation. Chemical compositions of these two fibers are illustrated in insets. Both fibers possess Ge-doped cores and only differ by the co-dopants used in their cladding.

reveals that these fibers can possess very different radiation sensitivities even with similar optical and structural properties before irradiation.

Most of the fibers studied in the literature are based on Total Internal Reflection (TIR) to ensure light guiding along the fiber (*mostly within the core and partially within the cladding*). This silica-based structure is surrounded by a polymer or metal-coating. The different silica layers constituting the medium for signal transmission are diversely doped to ensure that the resulting radial refractive-index profile (RIP) leads to light guidance. Different combinations of dopants can be used to obtain similar RIP structures, as illustrated in the insets of Fig. 5 for two COTS SM fibers responding to the ITU-T G.652 standard. This figure also compares for these two fibers the 1550 nm RIA growth during a 0.8 MeV neutron irradiation and the RIA changes after irradiation.

These results highlight that two COTS fibers with similar optical characteristics before irradiation can have extremely different responses to radiation. One fiber presents a limited RIA level of $\sim 1.5\ \mathrm{dB/km}$ at the end of the irradiation whereas the second fiber shows a linear increase of RIA, up to $\sim 14\ \mathrm{dB/km}$ for the same irradiation conditions. Furthermore, the more sensitive fiber exhibits no RIA bleaching after irradiation at room temperature whereas the other one partially recovers its transmission. Usually, the different characteristic parameters, such as the composition of COTS fibers shown in Fig. 5's insets, are considered as confidential by the fiber manufacturers. Consequently, the response of a COTS fiber to a radiative environment cannot easily be estimated without performing some radiation tests. The impact of the main incorporated dopants (Ge, F, P, N) on the fiber response will be further detailed in this paper.

B. Response of Microstructured Optical Fibers

Microstructured or photonic crystal optical fibers [24] are now also available for sensor applications. Two different types

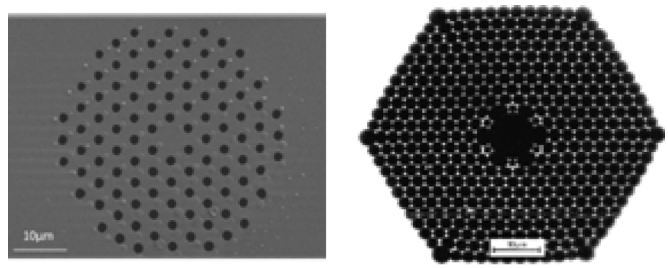

(a) (b)

Fig. 6. Illustrations of the structures of a) a TIR microstructured optical fiber [27] and b) a Hollow Core optical fiber [30].

of optical fibers are commercialized. The first one is a TIR solid core optical fiber with microstructured cladding [see Fig. 6(a)]. The second type is Hollow Core Fibers (HCF), illustrated in Fig. 6(b). The HCFs consists of an air-hole core surrounded by a microstructured cladding. For these fibers, the light guiding mechanisms are totally different from those of TIR fibers and currently result in a narrow transmission windows centered at wavelengths which depend on the structure parameters [24].

Only a few results are available concerning the radiation responses of microstructured optical fibers. For TIR solid core optical fibers, the RIA levels seem comparable to those of all-silica fibers made with the same glass [25]–[27]. On the contrary, HCFs present high radiation hardness under steady state γ-ray irradiation [28], [29] but more complex transient radiation responses under pulsed X-rays [30]. One of the interests of these fibers, in addition to their unique optical features, is that they can be made with only one glass type, which allows to reduce the complexity of the fiber response to radiations. Furthermore, the unique guiding properties of HCF can be used to harden the waveguide to radiation environments leading to compaction phenomenon in silica.

IV. Influence of the Fiber Composition on its Radiation Response

Optical fibers present a wide range of radiation sensitivities depending on the dopants used to design their refractive-index profiles. Furthermore, the amounts of impurities, such as chlorine Cl, also impact the device sensitivity (*eg. pure-silica core optical fibers generally have measurable amounts of OH and Cl in their cores, which has will be explained in this Section have notable effects on RIA*). Among the different dopants, the most used are Germanium (Ge), Phosphorus (P) and Nitrogen (N), which increase the glass refractive index, and Fluorine (F) or Boron (B) which decrease it. In the following, we review the main results concerning the responses of the most commonly used fiber types.

A. Pure-Silica Core (PSC) Optical Fibers

Some of the SM and MM optical fibers are designed with Pure Silica Core (PSC) and F-doping cladding. In this case, the fiber's refractive index presents a step-profile, which leads to a poor control of the dispersion properties of the waveguides. However, for applications that do not need an accurate control of this parameter, it has been shown that for most of the studied

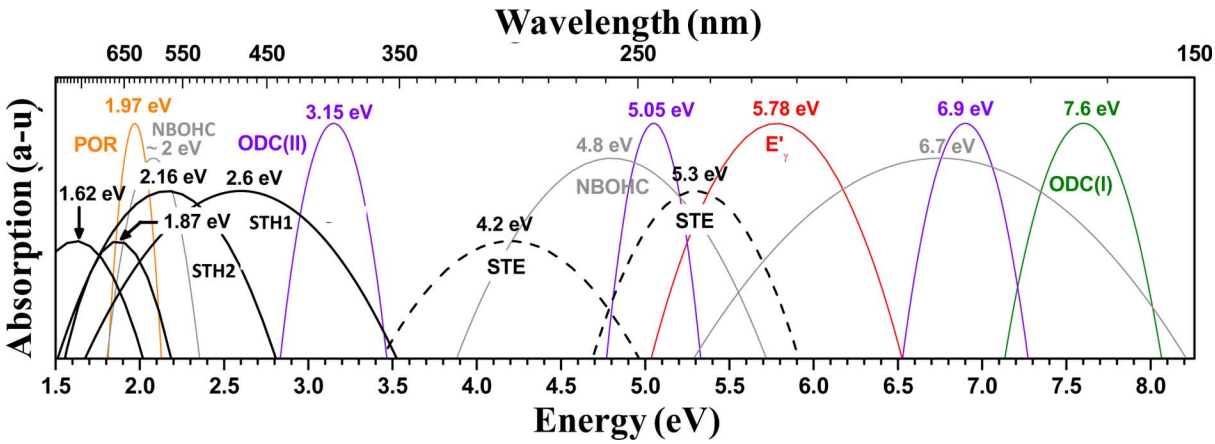

Fig. 7. Absorption bands associated with different Si-related point defect structures. More details concerning these defects can be obtained in the following references: SiE' centers, Peroxy Radicals (POR), oxygen deficient centers (ODC) and NBOHC in [42] and references therein. Absorption bands related to Self-Trapped Holes (STHs) have been extracted from [47]–[49] and those related to Self-Trapped Excitons (STE) from [51]. It is important to notice here that the bands associated with the STE defects will dominate the RIA spectra before their decay (typically below 1 ms after an irradiation pulse for $T < 170$ K), whereas a combination of the other bands will explain the RIA at times > 1 ms.

harsh environments this class of fibers presents the best radiation tolerance, along with some of the F-doped fibers. These fibers are characterized by low RIA levels from the UV to the IR part of the spectrum at doses exceeding 1 MGy) (however, very large RIA can be observed for lower doses and higher dose rates, unless the fiber has been pre-treated). A consequence of this good radiation tolerance in terms of RIA, is that the RIE phenomenon (mainly Cerenkov) can be easily observed in these fibers [31]. In this case, RIA and RIL phenomena are caused by Si-related point defects or by species related to the impurities. Recent reviews concerning these Si-related point defects can be found in, [12], [32]–[36].

In Fig. 7, we listed some of these defect structures that are associated with absorption bands in the silica gap. They have to be considered to understand the behavior of fibers under irradiation. As it can be seen, most of the studied point defects absorb in the UV and visible part of the spectrum. Today, only one possible absorption band related to the Self-Trapped Holes (STHs) has been pointed out in the IR (not represented in Fig. 7) [37].

The concentrations of these different point defects depend on various parameters such as the glass stoichiometry or the hydroxyl groups (OH) and Cl impurities contents, their amounts being correlated. Particularly, the amounts of Cl impurity strongly depend on the preform deposition technique used to elaborate the preforms, standard techniques authorize to reduce the OH groups concentration but the consequence is an increase of the amounts of Cl-related species;

Three main different classes of PSC fibers exist, depending on the manufacturing process and targeted range of wavelengths for the fiber operation. These three types of glasses possess different radiation responses:

- high-OH/low-Cl fibers, also called "wet" fibers
- low-OH/high-Cl fibers, also called "dry"fibers
- less commercially-available low-OH/low-Cl fibers.

Their vulnerability and relative interest strongly depend on the considered environments and on the application parameters, such as the operating wavelength. Their responses have been

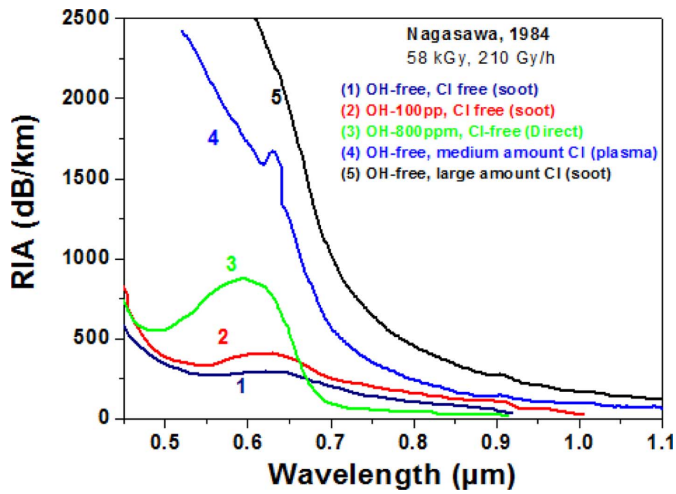

Fig. 8. Influence of the amounts of OH groups and Cl impurity on the γ-ray radiation response of pure-silica core fibers made by different processes. These data have been extracted from [46].

characterized under both continuous gamma and neutron irradiations [31], [38]–[40], and transient exposures [41].

For high dose environments (> 1 MGy), decreasing the Cl concentration is an efficient way to reduce the RIA in the UV and visible part of the spectrum. This is explained by the fact that the absorption bands of the Cl-related species are around 350 nm [42]–[46]. Both "wet" and low-OH/low-Cl fibers thus present interesting radiation responses in this range of wavelengths whereas "dry" fibers exhibit higher RIA levels. In low Cl concentration fibers, RIA is mainly due to the Non-Bridging Oxygen Hole Centers (NBOHC), which absorption bands are at 2 eV, 4.8 eV and 6.7 eV and at greater energies to the SiE' centers, which absorption band is around 5.78 eV [42]. This is illustrated in Fig. 8 which compares the spectral dependences of RIA measured in PSC optical fibers depending on their OH and Cl levels [46]. Different radiation hardening techniques, further detailed in this paper, have been studied to reduce the RIA induced by these particular defects.

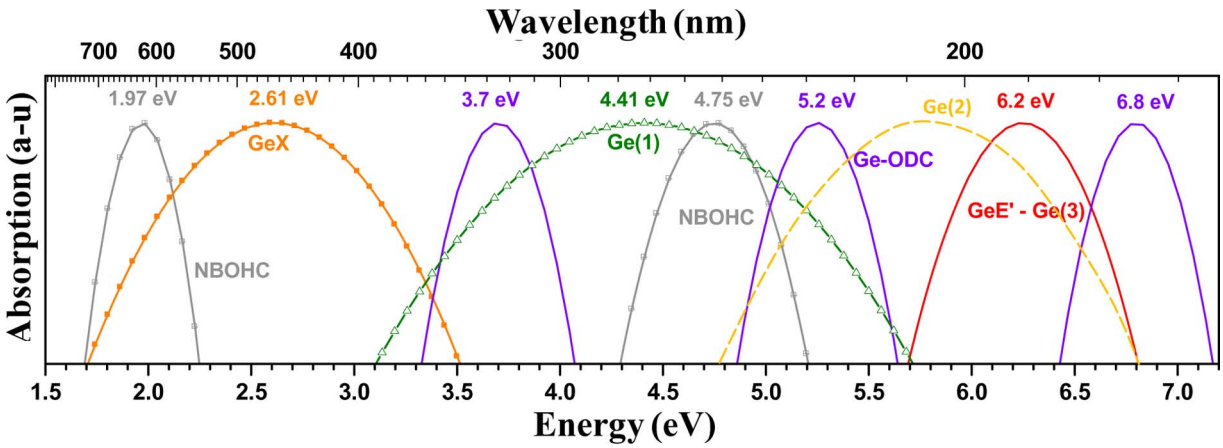

Fig. 9. Absorption bands associated with different Ge-related point defect structures. More details concerning the different point defects can be obtained in [61] and references therein.

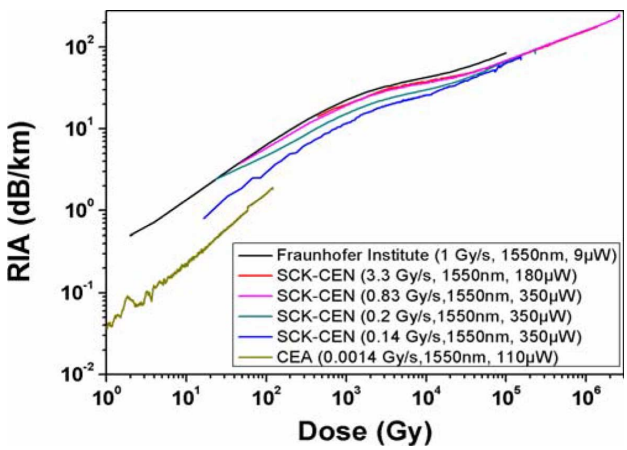

Fig. 10. RIA versus dose measured in the IR for SMF28 optical fibers, data compiled from unpublished CEA results and refs [56], [62], [63].

For lower doses (steady state or pulsed irradiations), it was shown that low-OH/low-Cl silica fibers present more complex radiation behaviors in the visible-infrared part of the spectrum, due to the contribution of STHs defects. The properties of these defects are discussed in details in the following [38], [47]–[49]. They are associated with various absorption bands peaking at wavelengths greater than 450 nm: 2.6 eV; 2.16 eV; 1.88 eV and 1.62 eV.

One of their particularities remains their overwhelming magnitudes during steady state irradiations at room temperature up to MGy doses above which radiation hardening mechanisms (see [40]) slowly begins to take place, reducing strongly their contribution to the observed RIA. As a consequence, they are less observed under steady state γ-rays during high dose irradiations, except at low temperatures or at the beginning of the irradiation run at ambient temperature [12], [50]. However, these defects are clearly visible during the first seconds after a pulsed irradiation as pointed out in [41] and this, even at room temperature. Their contribution, if any, seems to be lowered in "wet" samples or samples containing Cl impurity [41]. The transient optical absorption and luminescence induced by irradiation of amorphous SiO_2 with an electron pulse have been measured by Tanimura *et al.* [51] at low temperatures. The transient optical absorption spectra do not depend on impurities and have strong absorption bands peaking at 5.3 eV and 4.2 eV ascribed to self-trapped excitons (STE) or to a metastable excited state accompanied by a large lattice distortion. It is now assumed that self-trapped defects can act as precursor sites for the generation of optically active point defects during irradiation. The understanding of their contribution thus appears crucial for the design of radiation hardened optical fibers.

B. Germanosilicate Optical Fibers

There is a strong interest in the radiation responses of germanosilicate optical fibers, since most of the COTS Telecom-grade waveguides are of this type. This explains why Ge-doped fibers have been deeply evaluated for both radiation-tolerant telecommunication links [52], [53], space applications [54], high energy physics facilities, fusion by inertial [55] of magnetic confinement [56] and nuclear reactors [56]. These studies reveal that for most of the applications operating in the near-IR and IR (above 1 μm), Ge-doped fibers can be used, the RIA levels remaining acceptable. However, such fibers are characterized by very high radiation-induced losses in the UV, and RIA in the visible domain is considerably higher than in PSC fibers.

Spectroscopic studies reveal that in Ge-doped glasses, RIA and RIL are mainly explained by the contribution of Ge-related defects rather by the ones related to Si. Both experimental and theoretical studies confirm that Ge-related defects are more efficiently generated than Si-related defects [57]. Fig. 9 details some of the absorption bands tentatively associated with Ge-defect structures [57]. In addition to the research devoted to the understanding of radiation effects in this type of fibers, numerous studies have been performed on these defects to improve the understanding of the glass photosensitivity they induce [58]. This property is exploited for the inscription of Fiber Bragg Gratings (FBG) within these waveguides. The evaluation of the FBG radiation response is discussed in [59]. If for some of the Ge-related defects, strong correlations exist between defect structures

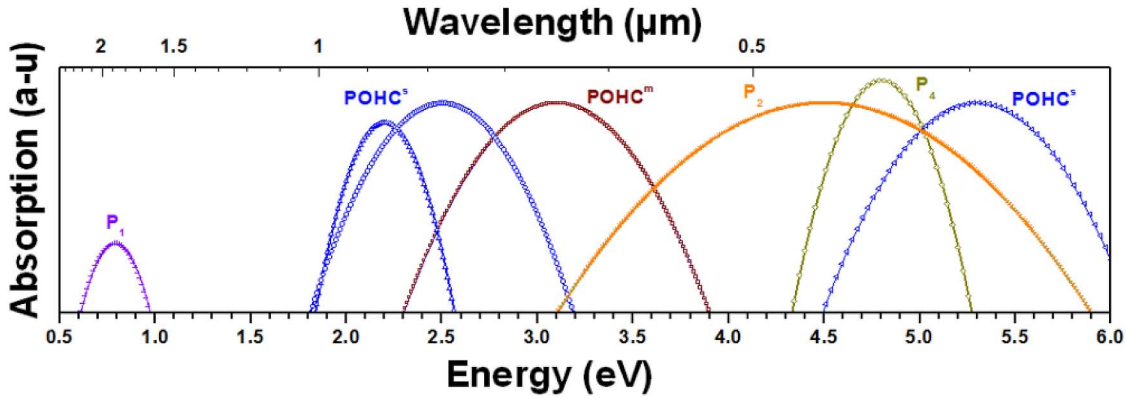

Fig. 11. Absorption bands associated with different P-related point defect structures. More details concerning the different point defects can be obtained in the following reference [67].

and optical properties, further studies, including the development of simulation tools, remain necessary to be able to associate some of the remaining absorption and luminescence bands to defect structures with confidence.

Except for low doses ($<$few tenths of kGy), the RIA in these fibers is larger than in PSC optical fibers. Various RIA growth and decay kinetics have been observed for Ge-doped cores but most of the observed differences can be explained by the influence of co-dopants like F or P, present in the fiber core and cladding [52], [53], [60]. The differences can be due to the generation of additional defects rather than Ge-related ones, such as P-related centers. They are also explained by the interactions between the different dopants that can affect the generation efficiency or the bleaching kinetics of Ge-related defects (case of F-co-doping).

Fig. 10 reviews different RIA measurements made by different research groups on the SMF28 optical fiber that possess a Germanium-doped core and a pure-silica-cladding. For a fiber containing only Ge, the RIA has been shown to monotonously increase with dose (D), up to a saturation level. This dose dependency can be modeled by a $C \times D^f$ growth law with exponent $f < 1$ and C corresponding to the defect growth. The different models used to reproduce the RIA time or dose dependence will be further detailed in the last part of this paper.

C. Phosphorus-Containing Optical Fibers

Phosphorus is often added as a co-dopant to silica-based optical fibers, due to its unique properties. It allows lowering the deposition temperature of a-SiO_2[64]. Its presence is also very useful in rare-earth doped optical fibers as it enhances the energy transfer efficiency between Yb^{3+} and Er^{3+} ions and thus maximizes the signal amplification in the 1550 nm output window [65]. Phosphorus is also used as the main dopant to optimize Raman fiber lasers [66] and amplifiers, or for other various sensor applications.

The presence of phosphorus induces the generation of several structures of point defects under irradiation. These defects have absorption bands in the visible and infrared part of the spectrum [67], as illustrated in Fig. 11. It should be noticed that this set of point defects allows us to reproduce RIA spectral dependency in the UV and visible part of the spectrum during and after γ-rays, X-rays or neutron irradiations [68] but fails in the near-IR and IR [69]. Most of these centers are stable at room temperature, which explains the well-known high radiation sensitivities of phosphosilicate glasses to continuous radiations. The stability and optical properties of these defects lead to a linear dose dependence of the RIA at several wavelengths and at low to moderate dose as well as an independence of these induced losses to dose rate or temperature [70].

These quite unique properties of P-doped fibers make them possible candidates for the development of radiation detectors [71] or dosimeters for various application fields [72], [73].

For applications having to operate during an irradiation pulse, the transient response of P-containing optical fibers is interesting since the P-related point defects are associated to lower RIA levels than the unstable Si or Ge-related defects at room-temperature [74]. However, this positive impact of P-doping is counterbalanced by the high level of permanent RIA measured after irradiation compared to other fibers classes. As a consequence, P-doped fibers may be useful for the design of time-resolved diagnostics for signal transmission during or just after the irradiation pulse but will be characterized by reduced lifetimes.

D. Nitrogen-Doped Optical Fibers

Fiber preforms containing nitrogen in the core have been synthesized by reduced-pressure plasma chemical deposition (SPCVD) and drawn into fibers [75]. Several studies have been conducted to evaluate the radiation vulnerability of this type of optical fiber. Under steady state irradiation, these fibers present low RIA levels in the IR, comparable to the levels measured for pure-silica core optical fibers, for doses up to 10 kGy.

At doses exceeding the MGy level, these fibers also present a good radiation tolerance with RIA slightly greater than for the radiation-hardened PSC fibers [76]. For transient exposures, N-doped optical fibers appear as very promising candidates for integration in time-resolved diagnostics, these fibers exhibiting the lowest transient RIA at both 1310 nm and 1550 nm [77]. Contrary to the P-doped optical fibers, their good transient response is not counterbalanced by high permanent RIA levels.

V. Influence of the Fiber Process Parameters and Other Extrinsic Parameters on its Radiation Response

A. Process Parameters

The fiber manufacturing generally consists in a two-step process. First, a preform is fabricated by successively depositing diversely doped layers on a rotating rod. Several techniques are used to fabricate the preforms, such as the OVD (outside vapor deposition process), the VAD (vapor axial deposition process), the MCVD (modified chemical vapor deposition process) and the PCVD (plasma CVD). Another technology, the Sol-Gel technique exists that can be used to obtain, for example, low-OH/low-Cl pure-silica core optical fibers.

In both cases, the resulting preform of typically a few cm in diameter is then drawn into a fiber having a diameter of about a few tenths or hundredths of microns. The drawing process is equivalent to a homothetic reduction of the preform, keeping unchanged, at a first order, the dopants and refractive-index profile distributions. During the drawing phase, a coating (polymer or metal) is applied to the fiber to ensure its mechanical resistance. Several parameters can be changed during the two phases to optimize the fiber transmission efficiency such as the stoichiometry of the glass, the temperatures of the deposition or drawing processes, the drawing speed and tension. Generally, since these different parameters are correlated, a strict study of the influence of one parameter is not easily possible.

As a consequence, less data is accessible concerning the influence of the process parameters (deposition and drawing) on the fiber radiation resistance compared to the composition influence. This is explained by the difficulties for researchers from the radiation effects community to have access to dedicated fiber (and preform) samples for this investigation. The most complete studies have been performed on samples elaborated by the modified chemical vapor deposition (MCVD) process and give insights on the influence of various parameters on RIA for this class of optical fiber. Friebele *et al.* present the first statistically robust study of the interrelationship of fiber parameters and steady state γ-ray RIA around 1300 nm in single mode germanosilicate optical fibers [52], [53]. The results on MCVD single-mode germanosilicate optical fibers have been completed by Girard *et al.* concerning their pulsed X-ray responses at 1310 and 1550 nm depending on various compositional, preform deposition temperature or drawing parameters [78]. More recently, the joint research team LabHC-CEA investigated the response of multimode MCVD optical fibers, providing evidence for the effect of the drawing process on the spectral dependence of the RIA and point defects generation for pure-silica core, fluorine-doped, germanium-doped and phosphorus-doped samples. The main results are that drawing increases the number of precursor sites for the optically-active point defect generation under irradiation but that changing the drawing parameters within the range of parameters usually covered for the elaboration of specialty optical fibers do not allow to minimize this effect. However, this also suggests that the definition of a radiation-tolerant fiber by MCVD will be robust against small production changes, an important advantage in terms of hardness assurance. Several studies are conducted in Russia to increase the radiation hardness of PCVD pure and N-doped optical fibers to MGy doses by optimizing the process parameters [77], [79], [80].

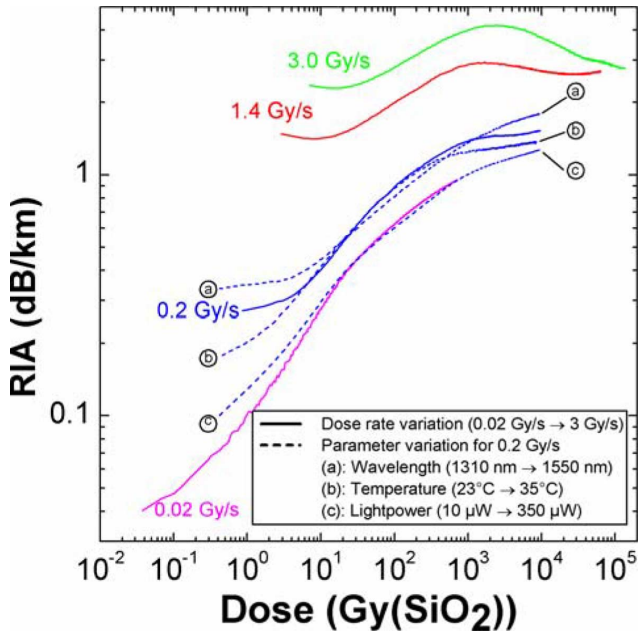

Fig. 12. Dose dependence of the RIA at 1310 nm in a fluorine-doped single-mode optical fiber (dose rate of 0.2 Gy/s). Influence of other parameters on the RIA growth law: temperature, injected light power, dose rate and wavelength. Data extracted from [94].

B. Other Fiber Parameters

Depending on the radiative constraints, other fiber parameters have been shown to impact the fiber radiation sensitivity. Among these different parameters, the nature of the coating has been investigated. For high neutron fluence, acrylate coating could be responsible for an increased RIA around 1380 nm due to the radiation induced radiolytic hydrogen from the polymer that diffuses to the fiber core. Hydrogen can then interact with the matrix to create OH groups, resulting in an increase in the OH overtone at 1.39 μm [81].

For pure-silica core fibers, it was shown that the use of silicone instead of F-doped cladding reduces the fiber degradation in the UV-visible linked to the conversion of Peroxy Linkages (POL) to NBOHCs under radiation [82]. The contribution of this mechanism to the fiber degradation also appears linked to the cladding to core diameters ratio (CCDR). In [83], the radiation sensitivity is decreased at smaller ratio. However, Kuhnehnn *et al.* showed that, in PSC fibers, the RIA dependence on coating material, CCDR, and core material depend on the production processes and can differ by up to a factor of 10 and even opposite to each other [84].

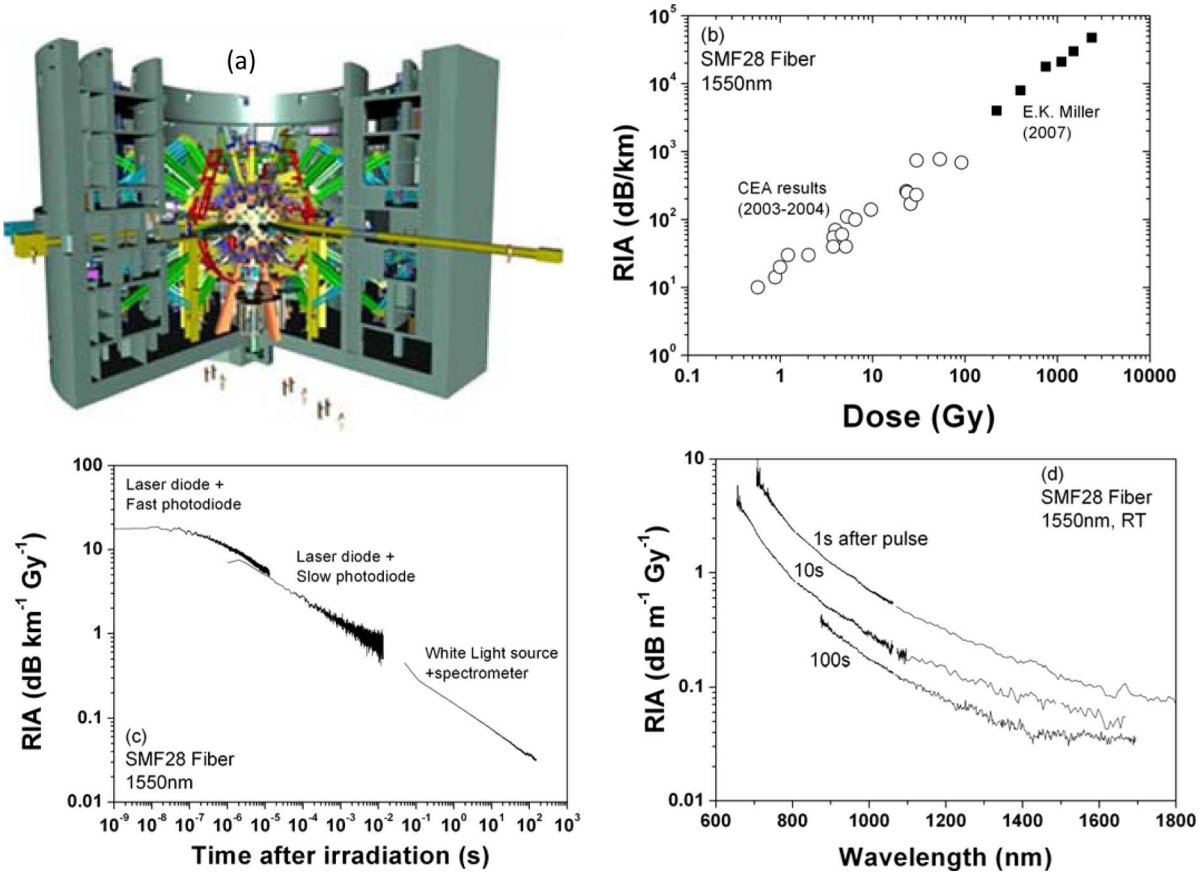

Fig. 13. (a) CAD drawing of the LMJ experimental area: the 10 m diameter target chamber is located at the center of the 30 m diameter experimental hall surrounded by the 2 m thick biological wall [74]. Results obtained for the single-mode SMF28 optical fiber (b) Dose dependence of the pulsed X-ray radiation-induced attenuation (RIA) peak measured at 1550 nm. This figure combines results obtained for both LMJ and NIF through different experiments at different radiation sources [110], [111]. (c) Time dependence of the RIA after the end of the X-ray pulse at 1550 nm, (d) Spectral dependences of the RIA measured at different times (1s, 10s, 100s) after the end of the X-ray pulse.

VI. Influence of the Radiative Environment Characteristics on the Fiber Radiation Response

A. Dose Dependence of RIA

Concentration of point defects and RIA levels generally increase with Total Ionizing Dose (TID). When investigating the dose dependence of the RIA at a given wavelength, a distinction should be made between pulsed and steady state irradiation. For continuous exposures, the growth kinetics of RIA with dose depends on the relative contribution of the generation rate and bleaching rate for the defects absorbing at the wavelength of interest. This results in various laws for the RIA vs Dose curves, from linear dose dependence for fibers presenting limited bleaching as P-doped fibers, to sub-linear growth for Ge-doped fibers (see Fig. 10) or more complex behaviors for pure-silica core or F-doped fibers (see Fig. 12) whose response is related to room temperature unstable defects. Detailed studies of the dose dependences in COTS SM and MM fibers can be found in [56] for the near-IR part of the spectrum and in [85]–[87] for COTS and prototype MM fibers and for the visible part of the spectrum.

Of course, this competition is also strongly dose rate dependent and both dose and dose rate effects are related. In this case, it appears that RIA can decrease at high doses, as illustrated in Fig. 12 when the bleaching rate of defects exceeds the generation rate (curve at 3 Gy/s). For pulsed (few ns) irradiations, the bleaching rate during the ns pulse is limited and a linear dose dependence of the RIA is observed [88] for fibers containing phosphorus or germanium. However, the dose dependence is not linear for PSC fibers, nor for fluorine-doped fibers.

B. Dose Rate Dependence of RIA and RIE

The vulnerability of an optical fiber is evaluated using the currently available facilities and often with accelerated testing at higher dose rate. The dose rate dependence of RIA has been evaluated to ensure the validity of these tests [89]. It was shown that for most of the fibers, the RIA increases with the dose rate. This is explained by the competition between the generation of point defects and their bleaching at the temperature of the experiments. When the dose rate increases, the defects are more rapidly generated and fewer defects are bleached during irradiation. Such dose rate dependence of RIA has been observed for pure-silica core optical fibers and germanosilicate fibers [90]–[92]. This dose rate dependence of the RIA at 1310 nm is illustrated in Fig. 12 for a fluorine-doped single-mode optical fiber that was fully characterized before integration in the LHC facility [93], [94].

More recently, some studies [95] pointed out a more complex dose rate dependence of RIA in certain types of rare-earth

doped optical fibers. For these fibers, it seems that an increase in RIA in the infrared is observed at lower dose rate. This larger degradation needs to be investigated in more details, but a possible analogy with the Enhanced Low Dose Rate Sensitivity (ELDRS) effect in electronics is suggested [95].

C. Temperature Dependence of RIA

Radiation induced changes strongly depend on the operating temperature, which strongly affects the stability of the optically-active defects. To benchmark different optical fibers with very tight constraints, even a few degrees difference leads to noticeable change in RIA [62]. If, at the first order, we could consider that the bleaching rate of point defects increases with temperature (see e.g., Fig. 12), its resulting effect on RIA at a given wavelength can be more complex due to the possible conversion from a defect structure to another one that could counterbalance this positive effect. Most of the recent studies devoted to temperature effects in optical fibers have been done in the $-50°\mathrm{C}$ to $100°\mathrm{C}$ range, which corresponds to the constraints of space applications, dosimetry or high energy physics applications.

Fewer papers investigate the response of optical fibers at more extreme temperatures, this research being driven by the targeted application constraints. Researchers from Princeton University [96], [97] measured the RIA and the RIE in different optical fibers submitted to radiations at various temperatures up to $400°\mathrm{C}$. The tested high-purity UV grade silica-silica fibers exhibited reduced RIA at $400°\mathrm{C}$, divided by a factor of at least 100 compared to room temperature (RT). However, operating at this high temperature has little or no effect on Cerenkov emission. Griscom [47] investigated the responses of fibers submitted to 77 K temperature, mainly to allow a better characterization of the point defects, like STHs that are known to be very unstable at RT. At this very low temperature, the RIA levels are strongly increased compared to the RT levels. Additional studies, not on optical fibers but rather on bulk samples are also of great interest to understand the temperature influence. For example, a complete study has been done by the Euratom/CIEMAT group in Madrid on bulk samples of pure-silica glasses irradiated at very high neutron fluences [98], [99]. From their analysis, it appears that Si-E', Si-ODC and Si-NBOHCs are bleached at temperatures exceeding $550°\mathrm{C}$. The temperature dependence of several radiation induced point defects have been studied in the literature by correlating different spectroscopic techniques. Very complete data is available for Si-related point defects [100], phosphorus defects [67] and Ge-related defects [101].

VII. Influence of the Application Parameters and Treatments on the Fiber Radiation Response

A. Wavelength, Injected Power

The RIA and RIE phenomena are strongly dependent on the wavelength of interest. This is explained by the various structures of point defects generated in the glass matrix that are associated with absorption bands centered at different wavelengths and with different full-widths at half maximum. Such dependence is illustrated in Figs. 8–13(d) that compare the radiation response measured in different optical fibers after steady state and transient irradiations. From a practical point of view, the wavelength choice (if any) of the application may be optimized to reduce the radiation sensitivity of a given optical fiber.

The injected light power might also influence the measured RIA. A higher light power can reduce the RIA level which is called photobleaching [102]. However, this effect is strongly reduced in modern telecommunication optical fibers [90].

B. Fiber History

The fiber radiation sensitivity is sometimes improved by applying pre-treatments before irradiation. Different pre-treatments were shown to be able to improve the radiation hardness of certain classes of optical fibers. However, none of them is universal, i.e., none of them is able to improve the hardness of all considered optical fibers. Most of the studies concerning pre-treatments have been done on pure-silica-core optical fibers that are very interesting candidates for most of the considered applications. The hydrogen or deuterium-loading can be very efficient to improve the fiber tolerance to radiation, since the H_2 or D_2 presence allows a more efficient and rapid passivation of the optically-active point defects [31], [103]. This point will be detailed in part VIII "Recent Advances". Another technique could be to pre-irradiate the fiber to convert the precursor sites into optically-active defects, then to apply a thermal or hydrogen treatment to bleach them. During the second irradiation, the number of precursor sites is reduced, as well as the RIA levels [38], [104].

VIII. Recent Advances

A. Fusion by Inertial Confinement: Megajoule Class Laser Projects

As illustrated in Fig. 1, the harsh environment associated with LMJ (or NIF) is characterized by a short duration pulse of complex nature. The radiative constraints include γ-rays, 14 MeV neutrons and hard X-rays [1]. Until recently and during the entire fiber vulnerability study by the CEA/LabHC joint research team (2004–2012), such a mixed pulse could only be obtained at the OMEGA facility, Rochester, USA [105]. Unfortunately, the OMEGA neutron yields per shot are lower by a factor of $\times 10^4$ compared to the ones expected for ignition shots at NIF or LMJ. The vulnerability studies were thus rather done by combining pulsed X-ray tests (Asterix pulsed generator at CEA [106]) with steady state experiments with 14 MeV or 0.8 MeV neutrons or γ-rays. To be able to extrapolate the results of these tests to the future LMJ or NIF environment, a good understanding of radiation effects and their microscopic origins is mandatory.

All the equipment located inside the experimental hall (EH) of the facility [Fig. 13(a)] will have to survive the radiations related to the different low or high-yield shots. 2 m-thick biological walls surrounding the EH ensure that radiations remain confined in this part of the facility. In case the fiber is used during or just after $(< 1\ \mathrm{s})$ irradiation, its transient response should be considered, as well as its permanent degradation induced by the succession of shots.

If the fiber-based system is only operated between successive shots, only the permanent degradation linked to the

cumulated TID or neutron fluence has to be considered. Different applications use fiber links in the EH (*tens of km*), from control-command applications to laser and plasma diagnostics. This wide variety increases the needed number of studies of the vulnerability of various passive optical fiber types (SM, MM, microstructured optical fibers), designed to work either in the UV-visible range of wavelengths or in the IR [27], [30], [41], [68], [69], [77], [107].

Irradiation tests have been achieved on both COTS optical fibers [108] and well-defined prototype samples [109], [110], resulting in a database of the different responses of COTS waveguides. This allows to understand the physics of radiation effects on fibers, to be able to imagine radiation hardening techniques. The vulnerability of these samples (RIA, RIE) has been experimentally characterized under irradiation. After irradiation, a complete set of spectroscopic techniques (*luminescence, absorption, confocal microscopy, electron paramagnetic resonance*) has been used to identify the radiation-induced point defects and their generation mechanisms.

Fig. 13 illustrates the dose per shot (b), time (c) and spectral (d) dependence of the RIA measured for the Corning SMF28 fiber, compiling measurements done by CEA for LMJ and by National Security Technologies for NIF [111]. With such measurements, we are able to estimate the fiber degradation for each location inside the EH and for each chronology of signal propagation inside a fiber link with respect to the irradiation shot. For most of the applications, COTS optical fibers present a sufficient radiation tolerance to ensure the functionality of data transmission during or after a shot and this for the facility lifetime.

There are several applications for which the radiative constraints are extremely high such as the fiber-based diagnostics operating in the UV and visible part of the spectrum [6]. To improve the radiation-hardness of COTS fibers, a coupled simulation/experiment approach has been developed between different research groups to design new fiber structures; it will be detailed in the last part of this paper devoted to "Future Challenges". In addition to these component characterizations, hardening-by-system techniques have been applied to reduce the exposition of the diagnostics to radiations, by optimizing the fiber links within the EH and by optimizing the fiber profile of use with respect to the mixed radiative pulse.

B. Fusion by Magnetic Confinement: Iter Project

ITER is an example of radiative environment which should be common in the future, fusion being considered as a prospect source of energy [112]. In tokamaks precise measurements of the plasma current and the magnetic field are essential to control the plasma magnetic equilibrium. In the current ITER scheme, the magnetic diagnostics have different designs but share one common feature: they are inductive sensors. Their operation relies on the generation of a voltage, resulting from a change in the magnetic field. The magnetic field is found by integrating the voltage over time. The use of such inductive sensors has a well-established record, including several tokamak implementations. However, time-derivative sensors have an inherent weakness for operation in a quasi-state regime. Until now that wasn't problem because the duration of plasma pulses in tokamaks is usually limited to tens of seconds, during which the plasma current varies significantly. In case of longer discharges, typically a few minutes, such as those obtained at Tore Supra, compensation techniques were developed to carry out precise measurements even with the presence of a relatively constant current [113]. In ITER the quasi-steady state operation goes together with high radiation levels. This radiation will disturb the operation of inductive sensors by inducing voltages in the cables due to ionization and insulation degradation. Considering this issue, plasma current measurements using methods based on non-inductive principles are required which opens perspectives for the development of fiber optic current sensors (FOCSs).

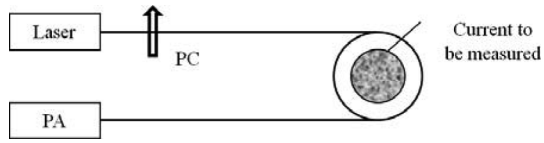

Fig. 14. General scheme of the FOCS. PC—polarization controller, PA—polarization analyzer.

The sentence stating that "optical fibers are inherently immune to electromagnetic interference" is almost a common place and travels from one publication to the other. This is actually not true. Optical fiber is indeed sensitive to electro-magnetic field when the polarisation properties are of concern. Operation of FOCS is based on the Faraday effect: magnetic field H aligned with the fiber axis creates circular birefringence in the fiber [114]. Fig. 14 illustrates a general scheme of the FOCS. A linearly polarized laser beam is launched into a single-mode fiber which makes loop(s) around a current; the fiber then returns to a detection system. The total polarization rotation ϕ is proportional to the integral of the magnetic field H over the fiber length. It follows from the Gauss theorem that the integral on a closed path in magnetic field is equal to the current flowing through the section. Therefore, the polarization rotation is proportional to the current enclosed by the optical fiber:

$$\phi = V \oint H \cdot dl = VI,$$

where the proportionality factor V is the Verdet constant.

The possibility to use a FOCS for MA-range plasma current measurement during long pulses was assessed on the Tore Supra tokamak [115]. Promising results have been obtained in terms of linearity with respect to the plasma current and long term stability of the measurements. At the same time, the linear birefringence was mentioned as a potential danger [114].

In ITER, the FOCS optical fiber can be placed on the external surface of the ITER vacuum vessel. The reference scenario of ITER operation corresponds to a 500 MW fusion power generation with a nominal integrated full power operation time of ~ 4700 h [116], [117]. At the FOCS fiber location, this corresponds to a total ionization dose of a few MGy and a total neutron fluence of 1.6×10^{18} n/cm^2. Such a high radiation load can cause significant RIA. However, FOCS relies on the polarimetric detection scheme, which is rather insensitive to transmission degradations. Induced optical losses up to 30–40 dB should have no major influence on the system performance.

The total FOCS fiber length exposed to the strong radiation field is ~ 15 m, which means that a RIA of up to 2–3 dB/m is acceptable. To demonstrate the radiation compatibility of the FOCS method fibers suited for FOCS applications (two of them were part of the test at Tore-Supra) were gamma-irradiated at dose-rate of 13 Gy/s up to a total dose of 2.5 MGy. The set of the tested fibers included: two low-Bi fibers, one with pure silica core and one with low-Ge doping; two spun fibers, one with low- and another with high-Ge doping; and two standard SMF-28 type fibers which were used as a [118]. The exact doping levels were not specified in [118]. The RIA remained below 0.5 dB/m either at 1550 or 1310 nm, which is compatible with the requirements above. A lowest RIA of 0.05 dB/m was observed in the low-birefringence pure silica fiber, which was explained as a consequence of the low dopant concentration and also a low internal stress [118].

Radiation can also influence the FOCS operation via material parameters change. Nuclear reactor radiation testing at neutron fluxes up to 2×10^{15} n/cm^2 ($E > 0.1$ MeV) did not show detectable Verdet constant modification. However, actual fluences will be an order of magnitude higher, and possible radiation effect on the Verdet constant needs to be studied. Additional research is also on-going to measure the poloidal magnetic field distribution using the FOCS fibers based on the combination of the Faraday effect and the optical reflectometry technology [119].

Thanks to their properties optical fibers are also viewed as a convenient waveguide technology to ease the design of optical system to be used in fusion. Optical fibers can be used for transporting visible and infrared light emitted by the thermonuclear plasma to remote diagnostic area where spectroscopy analysis is performed on the plasma light emission. Optical fiber can be very radiation resistant. However, considering the extreme radiation intensity expected in fusion reactors (typically a few MGy and fast neutron fluences of 10^{16}–10^{18} n/cm^2 depending on the location), additional radiation-hardening techniques have to be applied to mitigate the optical transmission vulnerability of fibers, especially at visible wavelengths where the RIA can quickly increase up to unacceptable values.

A possible approach proven to be efficient in reducing the RIA at visible wavelengths is to incorporate hydrogen into the fiber. The first experimental evidence of such radiation-resistant enhancement technology was shown by Faile [120] and Shelby [121] on bulk silica samples irradiated with ionizing radiation. Later, Nagasawa [122] applied the hydrogen loading technique on silica fibers and observed a reduction of the RIA by about a factor of two in the visible spectral range. Hydrogen is a light element, well-known to significantly modify the silica optical properties (absorption as well as refractive index). Hydrogen features the property of reducing the NBOHCs population—a defect responsible for the optical absorption in the visible spectral region (see Fig. 9) by converting them into hydroxyl groups (OH) with these latter absorbing light in the infrared spectral range (one overtone at 1390 nm) [121]. This reaction mechanism favors not only a decrease of the drawing induced absorption commonly observed in as-drawn fibers (mainly with low OH content) but also the RIA in the visible range in fibers with high or low OH content. The hydrogen-loading method has been

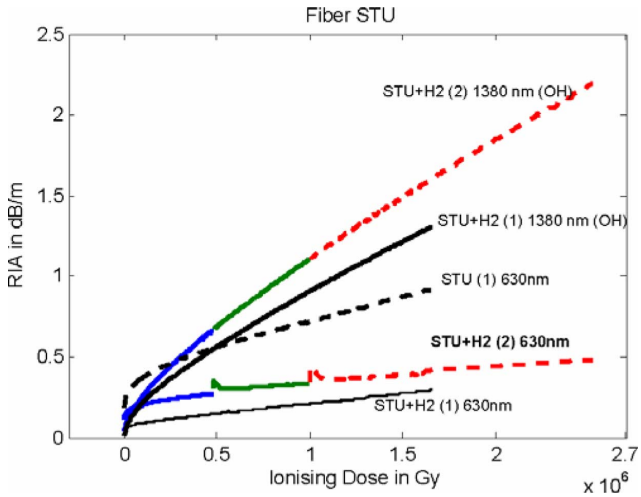

Fig. 15. RIA at 600 and 1380 nm in hydrogenated ($\mathrm{STU{+}H_2}$) and non-hydrogenated (STU) fibers. Marks (1) and (2) mean a first (6 Gy/s) and a second (4.2 Gy/s) irradiation, respectively. The second irradiation has been performed two years later in three successive steps.

applied to a low OH multimode fiber (STU preform, 200 μm core diameter) coated with aluminium to minimize the hydrogen losses by out diffusion. The STU fibers have a pure-silica core with low-Cl and low-OH and a F-doped cladding. The hydrogenated fiber has been irradiated under γ-rays (6 Gy/s) together with its hydrogen free counterpart. A similar second γ-ray irradiation (4.2 Gy/s) has also been conducted two years later on the same hydrogenated fiber to assess the evolution of the radiation resistance following long term storage at ambient temperature. Fig. 15 shows the result of the irradiation tests by comparing the RIA increase at 600 nm and 1390 nm in the hydrogenated and non-hydrogenated fibers. As expected, one can observe that the RIA at 600 nm is smaller in the hydrogenated STU fiber (by about a factor of 3) while the hydrogenated fiber $\mathrm{STU{+}H_2}$ (initial OH content is negligible) progressively accumulates more OH groups (larger RIA at 1390 nm). At the same time, one can also appreciate how effective is the aluminum coating in keeping the hydrogen inside the fiber since the RIA has only slightly increased after 2 years of storage at ambient temperature.

Similar hydrogenated fibers have also been irradiated in fission reactor irradiation conditions. Those severe irradiation tests (dose rate $>$ 300 Gy/s and fast neutron flux $> 10^{13}$ n $\cdot$ cm^{-2} $\cdot$ s^{-1}) have demonstrated a RIA lower than 1 dB/m at 630 nm for doses up to ~ 10 MGy and fast flux of 10^{17} n/cm^2 [123]. A possibility to further increase the radiation resistance is to use microstructured fibers whose porous media facilitates quick hydrogen diffusion through the holes [87], [124].

The hydrogen loading method has also proven to be efficient for irradiations in transient conditions. Fig. 16 shows the reduction of the RIA in the visible spectral region on hydrogenated and non-hydrogenated fibers either subjected to steady state gamma-rays (^{60}Co) or to pulsed X-rays irradiation.

Nevertheless, the major drawback of the hydrogen-loading method is that hydrogen progressively renders the fiber more sensitive to radiation for wavelengths below 475 nm (UV) for increasing dose (see Fig. 17). The cause of this effect is believed

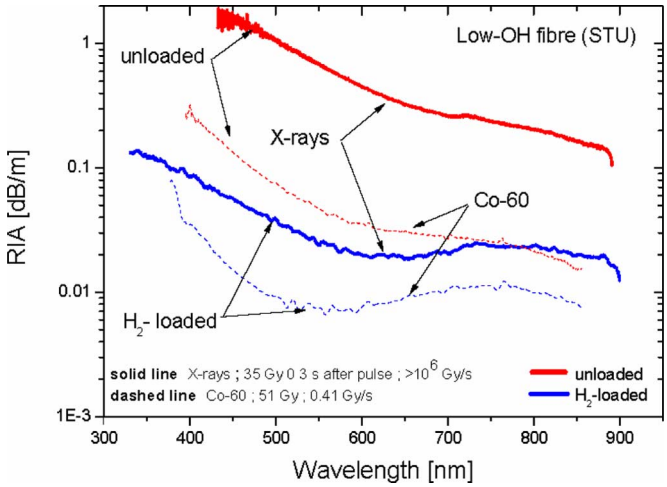

Fig. 16. Comparison of the pulsed X-ray (solid lines) and steady-state ^{60}Co (dashed lines) irradiation in a hydrogenated and non-hydrogenated (unloaded) low OH multimode fibers.

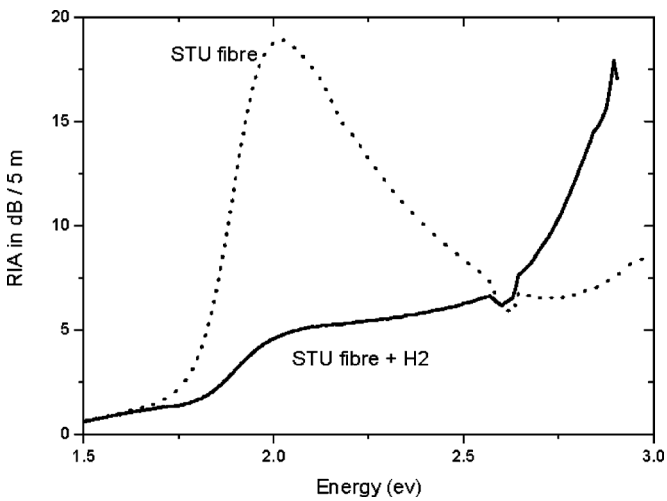

Fig. 17. RIA in hydrogenated ($\mathrm{STU}+\mathrm{H_2}$) and non-hydrogenated (STU) low OH fibers irradiated with gamma-rays up to 10 MGy (5.5 Gy/s). The graph shows the reduction of the absorption band in the hydrogenated fiber at energy around 2 eV while the RIA is enhanced for energy above 2.6 eV.

to originate from the creation of Si-ODC(II) defects which have an absorption band at 3.15 eV. The presence of Si-ODC(II) is indirectly evidenced by observing that photoluminescence (PL) increases in hydrogenated fibers as well as the H(I) concentration, whose Si-ODC is a precursor [125], [126].

To overcome this problem, a possible solution is to slightly dope the optical core with Fluorine. Indeed, lower RIA was generally observed below 500 nm in such fibers, compared to other low OH or hydrogenated fibers [31]. Fluorine tends to act in a similar way as hydrogen due to its high reactive capability: it blocks the formation of dangling bonds but without introducing optical absorption bands in the UV region. Nevertheless, fluorine is not as efficient as hydrogen in blocking the formation of NBOHCs and leads to higher RIA in the 600 nm region. In conclusion, a trade-off has to be applied in the choice of the fiber (hydrogen or fluorine doped) depending on the total expected dose and type of application (UV or visible).

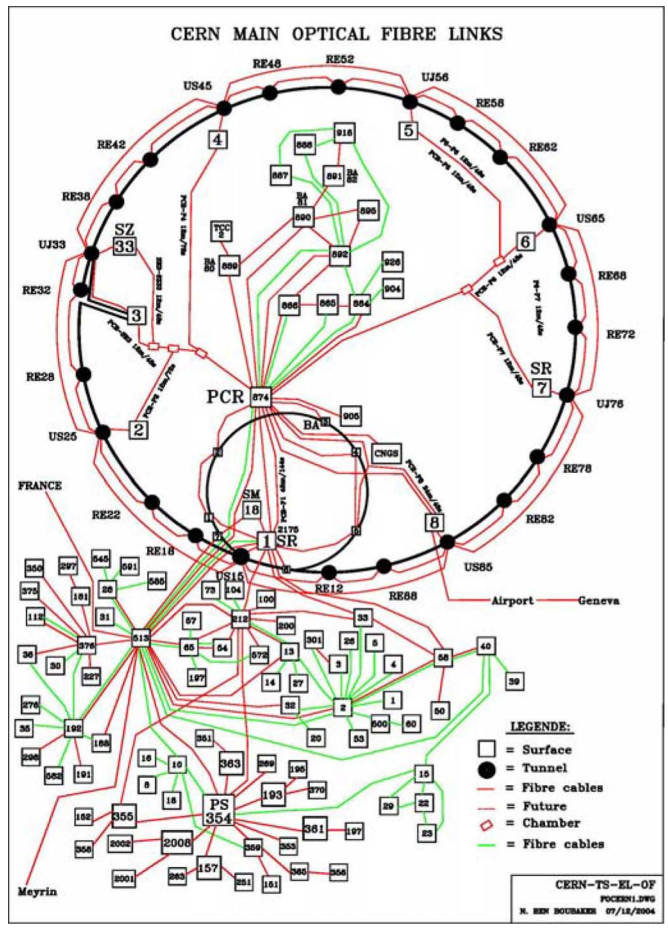

Fig. 18. Layout of main optical fiber links at CERN. Some of the fiber cables shown in red around the tunnel segments could be exposed to maximum dose rates up to 10 kGy/year [127].

C. Large Hadron Collider Project

The typical length of optical fibers used for signal transmission or sensor applications in radiation environments is relatively short, for example only some tenths of meters in satellites. One of the largest existing installations with optical fibers exposed to ionizing radiation is the Large Hadron Collider (LHC) project at CERN (Conseil Européen pour la Recherche Nucléaire), as illustrated in Fig. 18.

In the beam cleaning sections of this facility (designated as SZ33 and SR3 in Fig. 18), high doses (up to 100 kGy) were expected along fiber links of several hundreds of meters. The fibers to be selected for this environment had to be single-mode telecommunication fibers complying with ITU G.652B specifications. To avoid early failure of these links, a total induced attenuation below 6 dB/km was necessary implying the use of radiation hardened optical fibers.

By the time optical fibers needed to be installed in the tunnels, no market for large volumes of radiation resistant telecommunication fibers existed. For most of the former applications in radiation environments, carefully selected fibers were used, often produced by specialized companies or laboratories, that were able to deliver the needed short lengths. Equipping the LHC tunnel required more than 2500 km of fiber, exceeding the

production capabilities of most of the highly specialized manufacturers.

Consequently, to select the best suited fiber, not only the technical specifications (standard compliance, radiation hardness) were considered, but also the production capabilities, preform and fiber reproducibility, and availability of technical background information to assess the reliability.

The installation process was done in four steps: first, candidate manufacturers were invited to submit samples for a screening test done at the main wavelength of interest, at a moderate dose rate and at room temperature. Based on these results, two manufacturers supplied optimized products that were tested at different dose rates, wavelengths, temperatures and light powers (see Fig. 12 for examples of results) [93]. After that, one manufacturer was asked to deliver the total volume within one year. Since the radiation sensitivity of optical fibers may differ between products delivered by the same manufacturer, e.g., because he is utilizing production plants using different processes, a quality assurance procedure was implemented to closely follow the production process of the full batch. A fiber sample from each preform was irradiated and the resulting RIA was compared to the first sample provided by the manufacturer.

During this process, it turned out that the manufacturer changed details of the productions process to optimize the scheduled time of delivery. One consequence of this was a noticeable increase of the observed RIA values, so that countermeasures had to be implemented [62].

D. Space Applications

The studies of optical fibers vulnerability for integration in space missions show that most sensitive devices are the rare-earth doped and Polarization-Maintaining Fibers (PMFs), used for example in fiber optic gyroscopes. In this paper, we review the most recent studies regarding these two types of waveguides while a review of the response of telecom-grade optical fibers for space applications can be found in [128].

PMFs are necessary for applications that need to control the light polarization state during its propagation along the fiber, like in fiber optic gyroscopes. This control is obtained by introducing birefringence inside the waveguide. This birefringence can be produced by two basic mechanisms: geometrical shape birefringence or stress-induced birefringence resulting in very different fiber structures. The radiation responses of most of these structures have been characterized for both transient and continuous radiative environments.

The sensitivity of elliptical core fibers (geometrical shape birefringence) was measured at 1.3 μm and 1.55 μm under different irradiation conditions [129], [130]. Steady-state irradiation effects on PANDA fibers were described in [131], [133]. Radiation responses of fibers with elliptical stress were studied under both steady state [134] and pulsed irradiation [135].

The exact influence of PMF structure remains unclear. Some studies reported enhanced RIA levels and stability in PMF [136], [137], whereas others commented lower or similar RIA levels compared to standard SMFs with similar composition [130]. A future study with dedicated SM fibers and PMF is necessary to improve our knowledge of the relative role of PMF structure and composition. Recently, PMF with pure-silica core [138] and nitrogen [139] doped cores have been reported with enhanced radiation tolerance. Furthermore, the asymmetrical structure of a highly birefringent fiber could lead to differential RIA level between the two orthogonal polarization axes, as evidenced by Friebele *et al.* under steady-state irradiation [129] and following a radiation pulse [140]. This might have practical implications for example in fiber-optic gyroscopes, in which the polarization axis exhibiting the lowest RIA might be preferred. No evidence of this phenomenon was found in [130].

The case of Rare-Earth (RE) doped optical fibers is currently intensively studied, since a lot of possible applications exist: dosimetry, amplifiers, fiber lasers, high power sources. Among the different types of RE-doped fibers, Erbium (Er) and Er/Yt-terbium (Er/Yb)-doped fibers are the most studied [141]–[145] but other RE elements have also been considered in [146], [147]. The response of these fibers can be investigated under passive configurations similar to the ones used for passive fibers [141]–[144]. However, as most of the applications used these waveguides in an active scheme where the rare-earth ions are pumped in the near-IR to generate amplified signals in the IR, the most representative results are the ones obtained in active configurations [143], [148]–[151]. These studies first reveal a high sensitivity of COTS RE-doped optical fibers that explains their potential for dosimetry applications [152]. Spectroscopic measurements have shown that the excess losses are better explained by the nature of co-dopants (Aluminium, Phosphorus) used to facilitate RE incorporation rather than by the presence of the active ions. Furthermore, radiations at space levels seem to be associated with limited changes in the RE ions spectroscopic properties [153]. In recent years, different radiation hardening techniques have been suggested to enhance the radiation tolerance of RE fibers. Their RIA levels in the IR can be reduced by a H_2-preloading [154], [155], or by optimization of the pump wavelength [156]. Furthermore, Ce-co-doping of the glass has been recently shown to be very effective to reduce the fiber and amplifier radiation sensitivities for both Er/Yb [157] and Yb doped fibers [158], without strong degradation of the amplification efficiency [159]. Another possibility to increase the fiber radiation tolerance consists of using new deposition techniques allowing removing Al and P from the manufacturing process of Er-doped optical fibers [160]. In addition to the hardening of the fiber, the fiber amplifiers can also be hardened by design for a given space mission with the approach presented in [161].

E. Nuclear Power Plants Applications/Fiber Sensors

Industrial nuclear applications cover a wide range of radiation environments where optical fibers can be used for data transmission and sensing. From the point of view of radiation loads particularly demanding applications are reactor operation, spent fuel reprocessing, plant decommissioning and waste storage. In contrast to research installations like ITER or LHC, data transfer in such facilities is limited and optical fibers are not competing with the standard electrical wire data-transfer technology. The situation is changing for sensing applications, where optical fibers offer the possibility of distributed measurements, small size, passive operation, and remote interrogation,

which present significant benefits for the nuclear industry and potentially warrants the use of optical fiber sensors.

The idea to use optical fibers for distributed temperature measurements of large nuclear infrastructures such as reactor containment buildings, nuclear waste repositories and reactor primary circuitry was already proposed some time ago [162]–[164]. Radiation can compromise the performance of optical fiber sensors which design is not adjusted for radiation [165], even though there is no degradation of the underlying physical sensing mechanisms. For signal amplitude-based sensors, the RIA is definitely the main reason for performance degradation. The most straightforward and usually efficient approach to make such fiber systems radiation-tolerant is to use radiation-hardened fibers. Alternatively, systems relying on wavelength or polarisation encoded measurements may be, more robust. In some cases, the problem can be solved by applying compensation techniques. For example, in the standard distributed temperature measurements systems based on Raman scattering (optical phonons), temperature is derived from the ratio of the anti-Stokes to Stokes backscattered optical powers. The scattering location is defined from the time of flight of the probe pulse using optical time domain reflectometry. An attractive feature of the standard approach is that the fiber is interrogated from one end only. The measurements are not sensitive to the laser source power fluctuations. However, the ratio of the two powers depends on the fiber length, because of the difference in attenuation at the Stokes and anti-Stokes frequencies. This effect can be taken into account by calibration, but during irradiation, a spectral dependence of the RIA results in incorrect temperature estimations. To cope with spectral-dependent RIA, a simple double-end detection approach was demonstrated to be efficient [166]. In this configuration, the loop of sensing fiber was probed sequentially from the two ends. Temperature estimation was performed by calculating the mean of the two signals. This way, the effects of spectral-dependent optical losses in the fiber were eliminated, making the system insensitive to the RIA also. Simulation and experimental results have shown that the two-ended Raman distributed temperature measurements systems can perform satisfactorily under radiation, with doses up to 300 kGy, with an accuracy of $1^{\circ}\mathrm{C}$ [164].

Optical fiber distributed temperature measurements systems can also be based on Brillouin scattering (acoustic phonons). To address this possibility, effects of gamma-radiation up to a total dose of 10 MGy on the physical properties of Brillouin scattering in standard commercial optical fibers were studied [167], [168]. Frequency variations of $\sim 5\ \mathrm{MHz}$ for both the Brillouin frequency and the line-width were measured. Such a radiation-induced effect has a negligible practical impact and means that distributed sensors based on this interaction are potential candidates for the use in nuclear facilities.

Optical fibers can also be used for measurements of other environmental parameters. Dosimetry is obviously of particular interest for nuclear industry. In this case, the RIA is often considered as the underlying physical effect for on-line fiber-optic radiation monitoring, i.e., the amount of fiber darkening is the measure for a radiation dose absorbed by the fiber. Such fiber sensors are very small and therefore applicable to radio-therapy in-vivo dose deposition measurements [169].

The radiation sensitivity can be adapted by selecting suitably doped fiber. For dose ranges from tens of Gy to tens of kGy, phosphorous core doped fibers are suitable candidates [170]. An additional advantage of this type of fiber is a low annealing rate at room temperatures in the IR range.

In the case of radiotherapy, a sub-Gy sensitivity is necessary. Pb-doped fiber then appears to be a better choice. Polymethyl Methacrylate (PMMA) fibers have also been evaluated under irradiation [171]. They allow obtaining a broad radiation sensitivity range on one single fiber by interrogating it at multiple wavelengths in the visible spectrum.

The RIA-based point dosimetry can also be combined with an optical reflectometry technique which makes it suitable for surveillance of large scale nuclear facilities. The use of optical time-domain reflectometer (OTDR) technique for this purpose was proposed in the early 1980s [172] and further investigated in subsequent works [173]–[175].

However, practical realisation of such a system is confronted with issues such as the temperature dependence of RIA, saturation effects or dose-rate dependence. An OTDR dosimetry system operation was demonstrated at the DESY accelerator [176]. The distributed dose measurements were carried with a commercial OTDR, with a spatial resolution of $\sim 1.5\ \mathrm{m}$. A high dose resolution was obtained from 3 Gy to 1 kGy. The accelerator temperature environment was very stable, which allowed simplifying the system temperature calibration. In a general case, the RIA temperature dependence has to be taken into account, which presents a rather non-trivial task.

The spatial resolution can be improved down to the cm range for km-range interrogation by using Optical Frequency Domain Reflectometry (OFDR) based on Rayleigh scattering. A disadvantage of this approach is its high strain cross-sensitivity. The problem of cross-sensitivity is important for other fiber sensing techniques, but in this case it becomes especially acute. Combination of the OFDR with other techniques appears to be necessary.

Fiber optics dosimetry systems can also rely on light emission under irradiation. It can stem from Optically Stimulated Luminescence (OSL) [177] or from scintillating processes [178]. The former effect allows measuring the dose deposition down to cGy range while the latter is suited for high-bandwidth dose-rate measurements. OSL occurs thanks to optical excitation of carriers trapped on energy levels located in the band gap of the OSL crystal, followed by radiative decay. The process is induced by laser illumination, which provides the necessary optical stimulation. In the case of scintillation, the ionizing radiation excites atoms or molecules of a scintillating crystal which then de-excite via spontaneous radiative transitions. Light can also be generated via the Cerenkov effect. It was demonstrated that Cerenkov radiation can be used to monitor the reactor power and the high energy gamma-ray flux in a high neutron flux reactor [179]. Cherenkov detectors are also considered for the IFMIF facility [180].

A common disadvantage of all methods based on light emission is that distributed measurements are difficult to perform.

IX. Futures Challenges

A. Integrating the Fibers in Nuclear Environments

Implementing optical fiber for signal transmission or sensing applications in nuclear environments has always been a challenging task. With respect to the radiation hardness of fibers, the availability of test data from the manufacturers or distributors remains mostly limited. But, until recently, choosing a specific product after a careful assessment of its radiation response was at least a decision that lasted for a longer time period than currently, because the innovation cycles of optical fibers were rather long. Two decades ago, the main advancements in optical telecommunication involved the optimization of transceivers. For example the ITU recommendations for single-mode fibers G.652 remained essentially unchanged between 1984 and 2000 [181].

Recently, manufacturers introduced new technologies, e.g., for wavelength multiplexing, reduced polarization mode dispersion and bend insensitivity in case of single-mode fibers. Increasing demand for telecommunication bandwidth and concentration processes among the manufacturers lead to an increasing variation of products with short life cycles. To improve their products, manufacturers are constantly forced to optimize their processes and operate several plants around the world.

For applications in nuclear environments, this results in dramatic consequences: a tested fiber might not be available any longer, or might not be exactly the same product a year later. Products from the same manufacturer with the same designation might be produced at different sites using different processes. As a result, optically equivalent products from the same manufacturer could vary in their radiation response even from one order to the next one.

To overcome the risk of using different fibers for the final installation from the ones tested in a qualification process, the manufacturer needs to be aware of the special demands for nuclear applications. The radiation requirements need to be introduced in the selection as early as possible. A radiation quality assurance program should accompany the production process whenever possible [62]. The manufacturer should be made aware that changes that do not alter the standard specifications could make a product unusable in nuclear environments.

B. Needs for Multiscale Simulation for a Predictive Tool

Similarly as for radiation hardening of microelectronics where efficient simulation tools allow to reproduce the observed radiation response and to predict the vulnerability of future technology, such tools are crucially needed for fibers and fiber-based sensors. With such tools, the radiation responses of new fibers or the efficiency of radiation hardening techniques could be estimated with a reduced number of radiation tests.

Today, several empirical or semi-empirical models exist that predict the growth and decay kinetics of RIA versus the dose or time after irradiation when a sufficient amount of data is acquired on the considered fiber (see eg. [56], [85]. These tools are very useful to evaluate the fiber degradation at low dose rate from accelerated radiation testing results, eg. for space applications. The main models available in the literature are reviewed in Table I.

TABLE I
List of Published Models for Reproducing the RIA Growth and/or Decay Kinetics in Optical Fibers

Model type	Authors	Refs
Saturating exponentials	E.J. Friebele *et al.*	[182]
Power law	D.L. Griscom *et al.*	[89]
First and Second Order Fractal kinetics	D.L. Griscom	[92]
Stretched exponential fit	R.A.B. Devine	[183]
Series of superposable infinitesimal growth and decay events	D.T. H.Liu *et al.*	[184]
Saturated exponential curves with different relaxation + a dose dependent term	M. Kyoto *et al.*	[185]
β^{th}-order dispersive kinetic model	O. Gilard *et al.*	[95,186]
Complex first order fractal kinetics	Mashkov *et al.*	[187]
Saturated exponential curves + additional term	P.W. Levy	[188]
Kinetic order	H. Imai *et al.*	[189]
Kinetic Models	P. Borgermans *et al.*	[190]
Nth kinetic order	E.J. Friebele *et al.*	[191]

Recently, the development of more complete simulation tools becomes mandatory in order to overcome the challenges of developing radiation-tolerant optical fibers for plasma diagnostics of fusion-devoted facilities [192]. A long-term multi-scale simulation approach has then been suggested [108], [193] to respond to this need. This approach is illustrated in Fig. 19, as well as the different theoretical tools that are currently used at the different scales to model the glass or component response. As these tools are still under development, they have to be validated by comparison with experimental results collected over the last years on different samples, and acquired with the different techniques detailed in Fig. 19.

At atomic scale, *ab initio* calculations within the Density Functional Theory (DFT) framework can be used to calculate the structural and energy properties of point defects. With increasing calculation power, it becomes possible to simulate large supercells (eg. hundreds of atoms) and to statistically analyze the distribution of point defects properties due to the amorphous nature of silica [191]–[194]. With such cells, the study of dopant effects at concentrations exceeding 1 at% is possible; lower concentration implies the use of too large supercells at this time but such studies appear possible in the near future thanks to the development of new supercalculators, for example TERA 100 at CEA [195]. To get correct values for the bandgap or for the optical properties of point defects, codes beyond the DFT, such as the GW approximation and resolution of Bethe-Salpether equation are needed, treating the excited states [196], [197]. By coupling DFT and beyond DFT codes, we have shown, for the Si-ODC and Ge-ODC defects that optical properties of defect structures can be calculated [198]. Other techniques can be used to evaluate these optical properties, such as embedded cluster calculations [199], [200] or

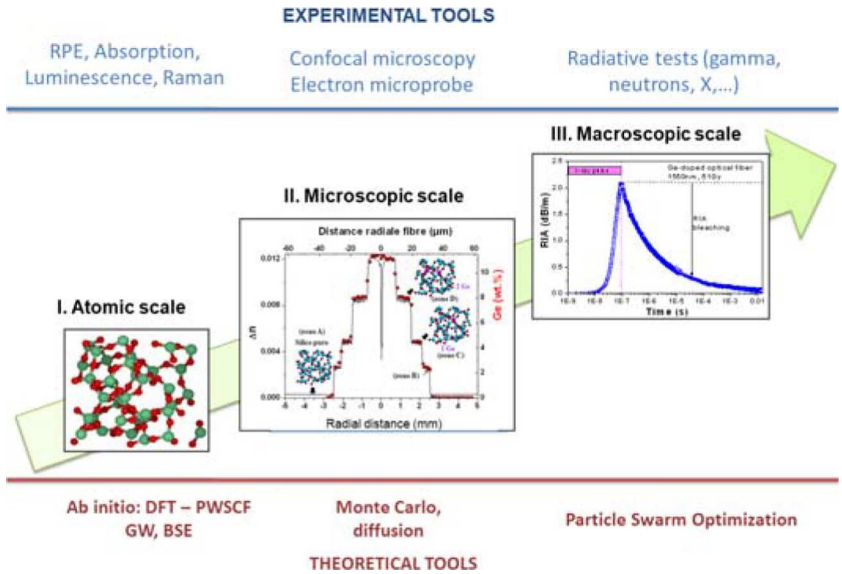

Fig. 19. Schematic representation of the coupled simulation/experiments approach used by the joint research team CEA-LabHC for the vulnerability and hardening studies of optical fibers and glasses.

quantum-chemical methods on clusters [201]. These techniques remain less adapted to the study of the statistical distribution of these properties. At microscopic scale, diffusion mechanisms of the mobile species, such as H_2, and their effects on the glass radiation sensitivity have to be considered, as well as the complex multilayers structure of fibers (*role of interfaces, stress distribution* …). Finally, the interaction of guided modes with the material has to be considered in order to determine the global response of the fiber through the RIA or RIE phenomena. This step implies coupling experimental results on the material response to simulation of the guiding properties of light inside the fiber. Different techniques allow us to calculate this modal distribution, even in complex fiber structures like double clad Er/Yb fibers or Hollow core fibers. At this time, such modeling has been done essentially for Rare-earth based optical fibers and amplifiers [161]. The different developed codes can be validated through comparison with experimental results from spectroscopic techniques such as Electron Paramagnetic Resonance (EPR), time or spatially-resolved luminescence or absorption, Raman spectroscopy …

C. Integration in Optical Links

Most optical fiber data communications and sensing applications also involve optical emitters and detectors with their associated electronics, and possibly other optical-fiber components such as couplers and Bragg grating filters, each of them having distinct radiation-sensitive properties. The two main radiation-matter effects, i.e., ionization and knock-on effects, also result in two different trends.

Cumulated ionizing doses typically cause increased noise levels in detectors and voltage level shifts in electronic circuits, which may vary depending on the involved semiconductor materials and their layout. Gamma radiation hardly affects quantum-based optical emitters, provided their packaging avoids doped focusing lenses.

Energetic particles tend to increase threshold currents of laser diodes and diminish their emission efficiency through the creation of non-radiative defect centers in their optically active region. Similarly, detectors see their efficiency decreasing, while their noise levels usually grow even more significantly than under gammas. Moreover, charged particles also induce single events through local deposition of energy. They are merely detrimental in digital circuitry of optical links, and even more so as transmission rates increase.

In summary, increasing noise levels and laser thresholds, possible wavelength shifts and single events all affect the optical link in terms of reduced optical budget and available bandwidth, if not considered carefully with respect to the expected environment. Fortunately, the recent industrial-driven miniaturization of these opto-electronics resulted in more robust components, mainly regarding their total dose robustness, which is a volumetric effect, typically observed in isolating oxide structures. This tendency to diminish active volumes however strengthened their vulnerability to single event effects, since the same amount of locally deposited energy has a relatively larger effect.

X. Conclusion

We reviewed in this paper the recent advances in the field of radiation effects on optical fibers, giving the key results of the most recent studies conducted in the framework of the LMJ, ITER, LHC, nuclear industries and space projects. Thanks to the new available classes of optical fibers, as well as thanks to radiation hardening techniques, optical fibers can survive the harsh environments associated with most of these applications. However, for the most challenging needs, deeper knowledge of radiation effects on silica-based matrix remains necessary to be able to access predicting simulation tools and to authorize the development of fiber or fiber-based sensors for future applications. Thanks to the growing interest of the nuclear industry in fiber-based sensors, studies are in progress around the world to overcome these challenges and to enhance fiber integration in radiative environments.

ACKNOWLEDGMENT

The would like to thank Richard, J. Baggio, P. Paillet, M. Gaillardin, M. Raine from CEA, V. Ferlet-Cavrois from ESA, J.-P. Meunier, B. Tortech, J. Bisutti, G. Origlio, M. Vivona, A. Alessi, L. Vaccaro, X. Phéron, A. Morana, D. Di Franscesca, M. Léon from LabHC, H. Henschel, S. Hoeffgen from Fraunhofer Institute, and T. Wijnands from CERN for fruitful discussions. Part of the presented results was acquired in the framework of the joint research team (ERC) between CEA and Saint-Etienne.

REFERENCES

[1] J.-L. Bourgade, V. Allouche, J. Baggio, C. Bayer, F. Bonneau, C. Chollet, S. Darbon, L. Disdier, D. Gontier, M. Houry, H.-P. Jacquet, J.-P. Jadaud, J.-L. Leray, I. Masclet-Gobin, J.-P. Negre, J. Raimbourg, B. Villette, I. Bertron, J. M. Chevalier, J.-M. Favier, J. Gazave, J.-C. Gomme, F. Malaise, J.-P. Seaux, V. Y. Glebov, I. P. Jaanimag, C. Stoeckl, T. C. Sangster, G. Pien, R. A. Lerche, and E. R. Hodgson, "New constraints for plasma diagnostics development due to the harsh environment of MJ class lasers," *Rev. Sci. Instrum.*, vol. 75, no. 10, pp. 4204–4212, 2004.

[2] J. Troska, G. Cervelli, F. Faccio, K. Gill, R. Grabit, R. M. Jareno, A.-M. Sandvik, and F. Vasey, "Optical readout and control systems for the CMS tracker," *IEEE Trans. Nucl. Sci.*, vol. 50, no. 4, pp. 1067–1072, Aug. 2003.

[3] P. W. Marshall, C. J. Dale, and K. A. LaBel, "Space radiation effects in high performance fiber optic data links for satellite data management," *IEEE Trans. Nucl. Sci.*, vol. 43, no. 2, pp. 645–653, Apr. 1996.

[4] C. Barnes, L. Dorsky, A. Johnston, L. Bergman, and E. Stassinopoulos, "Overview of fiber optics in the natural space environment," in *Proc. SPIE Fiber Optics Reliability: Benign and Adverse Environments IV*, 1990, vol. 1366, pp. 9–16.

[5] T. Kakuta, T. Shikama, T. Nishitani, B. Brichard, A. Krassilinikov, A. Tomashuk, S. Yamamoto, and S. Kasai, "Round-robin irradiation test of radiation resistant optical fibers for ITER diagnostic application," *J. Nucl. Mater.*, vol. 307–311, pp. 1277–1281, 2002.

[6] G. M. Ermolaeva, M. A. Eronyan, K. V. Dukelskii, A. V. Komarov, Y. N. Kondratev, M. M. Serkov, M. N. Tolstoy, V. B. Shilov, V. S. Shevandin, H. T. Powell, and C. E. Thompson, "Low-dispersion optical fiber highly transparent in the UV spectral range," *Opt. Eng.*, vol. 43, pp. 2896–2903, 2004.

[7] A. Fernandez-Fernandez, "Photonics for Nuclear Environments From Radiation Effects to Applications in Sensing and Data-Communication," Ph.D. dissertation, Faculté Polytechnique de Mons, Mons, 1997.

[8] D. Sporea, A. Sporea, S. O'Keeffe, D. McCarthy, and E. Lewis, "Optical fibers and optical fiber sensors used in radiation monitoring," *Sel. Top. Opt. Fiber Technol., In Tech*, Feb. 2012.

[9] A. Fernandez-Fernandez, H. Ooms, B. Brichard, M. Coeck, S. Coenen, F. Berghmans, and M. Décreton, "SCK-CEN Gamma irradiation facilities for radiation tolerance assessment," in *Proc. NSREC Data Workshop*, 2002, pp. 171–176, 02HT8631.

[10] E. J. Friebele, "Optical fiber waveguides in radiation environments," *Opt. Eng.*, vol. 18, pp. 552–561, 1979.

[11] E. J. Friebele, G. C. Askins, M. E. Gingerich, and K. J. Long, "Optical fiber waveguides in radiation environments, II," *Nucl. Instrum. Meth. Phys. Res. B*, vol. 1, no. 2–3, pp. 355–369, 1984.

[12] B. Brichard and A. Fernandez-Fernandez, A. F. Fernez, Ed., "Radiation effects in silica glass optical fibers," in *RADECS 2005 Short Course, New challenges for Radiation Tolerance Assessment*, 2005.

[13] R. A. B. Devine, J.-P. Duraud, and E. Dooryhee*, Structure and Imperfections in Amorphous and Crystalline Dioxide*. Chichester, U.K.: Wiley, 2000.

[14] W. H. Zachariasen, "The atomic arrangement in glass," *J. Am. Chem. Soc.*, vol. 54, no. 10, pp. 3841–3851, 1932.

[15] R. J. Bella and P. Dean, "The structure of vitreous silica: Validity of the random network theory," *Philosoph. Mag.*, vol. 25, no. 6, pp. 1381–1398, 1972.

[16] A. C. Wright, "Defect-free vitreous networks: The idealized structure of SiO_2 and related glasses," in *Defects in* SiO_2 *and Related Dielectrics:Science and Technology*, G. Pacchioni, L. Skuja, and D. L. Griscom, Eds. Dordrecht, The Netherlands: Kluwer, 2000.

[17] D. L. Griscom, "Intrinsic and extrinsic point defects in a-SiO_2," in *The Physics and Technology of Amorphous* SiO_2, R. A. B. Devine, Ed. New York: Plenum, 1988, pp. 125–134.

[18] D. L. Griscom, "Nature of defects and defect generation in optical glasses," in *Proc. SPIE. 541 "Radiation Effects in Optical Materials"*, 1985, pp. 38–59.

[19] T. P. Ma and P. V. Dressendorfer*, Ionizing Radiation Effects in MOS Devices and Circuits*. New York: Wiley-Interscience, 1989.

[20] W. Primak, "Fast-neutron-induced changes in quartz and vitreous silica," *Phys. Rev. B*, vol. 110, no. 6, pp. 1240–1254, 1958.

[21] E. Lell, N. J. Hensler, and J. R. Hensler, J. Burke, Ed., "Radiation effects in quartz, silica and glasses," in *Progr. Ceramic Sci.*, New York, 1966, vol. 4, pp. 3–93, Pergamon.

[22] A. F. Fernandez, B. Brichard, S. O'Keeffe, C. Fitzpatrick, E. Lewis, J.-R. Vaille, L. Dusseau, D. A. Jackson, F. Ravotti, M. Glaser, and H. El-Rabii, "Real-time fibre optic radiation dosimeters for nuclear environment monitoring around thermonuclear reactors," *Fusion Eng. Des.*, vol. 83, no. 1, pp. 50–59, 2008.

[23] S. O'Keeffe, A. F. Fernandez, C. Fitzpatrick, B. Brichard, and E. Lewis, "Real-time gamma dosimetry using PMMA optical fibres for applications in the sterilization industry," *Meas. Sci. Technol.*, vol. 18, pp. 3171–3176, 2007.

[24] P. Russell, "Photonic crystal fibers," *Science*, vol. 299, pp. 358–362, 2003.

[25] S. Girard, A. Yahya, A. Boukenter, Y. Ouerdane, J.-P. Meunier, R. E. Kristiansen, and G. Vienne, "Gamma radiation-induced attenuation in photonic crystal fibre," *IEE Electron. Lett.*, vol. 38, no. 20, pp. 1169–1171, 2002.

[26] A. F. Kosolapov, I. V. Nikolin, A. L. Tomashuk, S. L. Semjonov, and M. O. Zabezhailov, "Optical losses in as prepared and gamma-irradiated microstructured silica-core optical fibers," *Inorg. Mater.*, vol. 40, no. 11, pp. 1229–1232, 2004.

[27] S. Girard, Y. Ouerdane, M. Bouazaoui, C. Marcandella, A. Boukenter, L. Bigot, and A. Kudlinski, "Transient radiation-induced effects on solid core microstructured optical fibers," *Opt. Exp.*, vol. 19, pp. 21760–21767, 2011.

[28] H. Henschel, J. Kuhnhenn, and U. Weinand, "High radiation hardness of a hollow core photonic bandgap fiber," presented at the 8th Eur. Conf. Radiation and its Effects on Components and Systems, RADECS 2005, 2005, paper LN4.

[29] G. Cheymol, H. Long, J. F. Villard, and B. Brichard, "High level gamma and neutron irradiation of silica optical fibers in CEA OSIRIS nuclear reactor," *IEEE Trans. Nucl. Sci.*, vol. 55, no. 4, pp. 2252–2258, Aug. 2008.

[30] S. Girard, J. Baggio, and J.-L. Leray, "Radiation-induced effects in a new class of optical waveguides: The air guiding photonic crystal fibers," *IEEE Trans. Nucl. Sci.*, vol. 52, no. 6, pp. 2683–2688, Dec. 2005.

[31] B. Brichard, A. F. Fernandez, H. Ooms, F. Berghmans, M. Decreton, A. Tomashuk, S. Klyamkin, M. Zabezhailov, I. Nikolin, V. Bogatyrjov, E. Hodgson, T. Kakuta, T. Shikama, T. Nishitani, A. Costley, and G. Vayakis, "Radiation-hardening techniques of dedicated optical fibres used in plasma diagnostic systems in ITER," *J. Nucl. Mater.*, vol. 329–333, pp. 1456–1460, 2004.

[32] L. Skuja, "Optically-active oxygen-deficiency-related centres in amorphous silicon dioxide," *J. Non-Cryst. Solids*, vol. 239, no. 1–3, pp. 16–48, 1998.

[33] M. Cannas, "Point Defects in Amorphous SiO2: Optical Activity in the Visible, UV and Vacuum-UV Spectral Regions," Ph.D. dissertation, Università di Palermo, Palermo, Italy, 1998.

[34] S. Agnello, "Gamma Ray Induced Processes of Point Defect Conversion in Silica," Ph.D. dissertation, Università di Palermo, Palermo, Italy, 2000.

[35] G. Buscarino, "Experimental investigation on the microscopic structure of intrinsic paramagnetic point defects in amorphous silicon dioxide," Ph.D. dissertation, Università di Palermo, Palermo, Italy, 2007.

[36] L. Skuja, M. Hirano, H. Hosono, and K. Kajihara, "Defects in oxide glasses," *Phys. Stat. Sol. (c)*, vol. 2, no. 1, pp. 15–24, 2005.

[37] P. V. Chernov, "Spectroscopic manifestations of self-trapped holes in silica," *Phys. Stat. Sol.*, vol. B115, pp. 663–675, 1989.

[38] D. L. Griscom, "Radiation hardening of pure-silica-core optical fibers: Reduction of induced absorption bands associated with self-trapped holes," *Appl. Phys. Lett.*, vol. 71, pp. 175–177, 1997.

[39] A. L. Tomashuk, E. M. Dianov, K. M. Golant, and A. O. Rybaltovskii, "γ-radiation-induced absorption in pure-silica-core fibers in the visible spectral region: The effect of H2-loading," *IEEE Trans. Nucl. Sci.*, vol. 45, no. 3, pp. 1576–1579, Jun. 1998.

[40] D. L. Griscom, "γ and fission-reactor radiation effects on the visible-range transparency of aluminum-jacketed, all-silica optical fibers," *J. Appl. Phys.*, vol. 80, pp. 2142–2155, 1996.
[41] S. Girard, D. L. Griscom, J. Baggio, B. Brichard, and F. Berghmans, "Transient optical absorption in pulsed-X-ray-irradiated pure-silica-core optical fibers: Influence of self-trapped holes," *J. Non-Cryst. Solids*, vol. 352, no. 23–25, pp. 2637–2642, 2006.
[42] L. Skuja, "Optical properties of defects in silica," in *Defects in* SiO_2 *and Related Dielectrics: Science and Technology (NATO Science Series II)*, G. Pacchioni, L. Skuja, and D. L. Griscom, Eds. Dordrecht, The Netherlands: Kluwer, 2000, pp. 73–116.
[43] D. L. Griscom, E. J. Friebele, and S. P. Mukherjee, "Studies of radiation-induced point defects in silica aerogel monoliths," *Cryst. Latt. Def. and Amorph. Mat.*, vol. 17, pp. 157–163, 1987.
[44] E. M. Dianov, L. S. Kornienko, A. O. Rybaltovskii, and P. Chernov, "Unstable radiation colour centres in pure silica fibres: The nature and properties," *Proc. SPIE*, vol. 2425, pp. 148–154, 1994.
[45] H. Mori, Y. Suzuki, and M. Hirai, "Selective photobleaching of radiation- induced absorption in a-SiO_2," *Nucl. Instrum. Meth. Phys. Res. B*, vol. 91, pp. 391–394, 1994.
[46] K. Nagasawa, M. Tanabe, and K. Yahagi, "Gamma-ray-induced absorption bands in pure-silica-core fibers," *Jpn. J. Appl. Phys.*, vol. 23, pp. 1608–1613, 1984.
[47] D. L. Griscom, "γ-Ray-induced visible/infrared optical absorption bands in pure and F-doped silica-core fibers: Are they due to self-trapped holes?," *J. Non-Cryst. Solids*, vol. 349, pp. 139–147, 2004.
[48] D. L. Griscom, "Self-trapped holes in pure-silica glass: A history of their discovery and characterization and an example of their critical significance to industry," *J. Non-Cryst. Solids*, vol. 352, pp. 2601–2617, 2006.
[49] Y. Sasajima and K. Tanimura, "Optical transitions of self-trapped holes in amorphous SiO_2," *Phys. Rev. B*, vol. 68, pp. 014204–014204, 2003.
[50] B. Brichard, M. Van Uffelen, A. F. Fernandez, F. Berghmans, M. Décreton, E. Hogdson, T. Shikama, T. Kakuta, A. Tomashuk, K. Golant, and A. Krasilnikov, "Round robin evaluation of optical fibres for plasma diagnostics," *Fusion Eng. Des.*, vol. 5–57, pp. 917–921, 2001.
[51] K. Tanimura, C. Itoh, and N. Itoh, "Transient optical absorption and luminescence induced by band-to-band excitation in amorphous SiO_2," *J. Phys. C: Solid State Phys,.*, vol. 21, pp. 1869–1876, 1988.
[52] E. J. Friebele, Correlation of Single Mode Fiber Fabrication Factors and Radiation Response 1991, Final Rep., NRL/MR/6505-92-6939.
[53] E. J. Friebele, C. G. Askins, C. M. Shaw, M. E. Gingerich, C. C. Harrington, D. L. Griscom, T.-E. Tsai, U.-C. Paek, and W. H. Schmidt, "Correlation of single-mode fiber radiation response and fabrication parameters," *Appl. Opt.*, vol. 30, pp. 1944–1957, 1991.
[54] M. Ott, "Radiation effects data on commercially available optical fiber: Database summary," in *Proc. IEEE NSREC Data Workshop*, 2002, pp. 24–31.
[55] J. Bisutti, "Etude De La Transmission Du Signal Sous Irradiation Transitoire Dans Les Fibres Optiques," Thèse de Doctorat, Université de Saint-Etienne, Saint-Etienne, France, 2010.
[56] M. Van Uffelen, "Modélisation de Systèmes D'acquisition Et De Transmission à Fibres Optiques Destinés à Fonctionner En Environnement Nucléaire," Thèse de Doctorat, Université de Paris XI, Paris, 2001.
[57] V. B. Neustruev, "Colourcentres in germanosilicate glass and optical fibres," *J. Phys.: Condens. Matter*, vol. 6, pp. 6901–6936, 1994.
[58] K. O. Hill, B. Malo, F. Bilodeau, and D. C. Johnson, "Photosensitivity in optical fibers," *Annu. Rev. Mater. Sci.*, vol. 23, pp. 125–157, 1993.
[59] A. Gusarov, S. Höffgen, and J. Kuhnhenn, "Radiation effects on fiber Bragg gratings," *IEEE Trans. Nucl. Sci.*, to be published.
[60] S. Girard, J. Keurinck, Y. Ouerdane, J.-P. Meunier, and A. Boukenter, "Gamma-rays and pulsed X-ray radiation responses of germanosilicate single-mode optical fibers: Influence of cladding codopants," *J. Lightw. Technol.*, vol. 22, pp. 1915–1922, 2004.
[61] A. Alessi, "Germanium Point Defects induced by Irradiation in Ge-Doped Silica," Ph.D. dissertation, Università di Palermo, Palermo, Italy, 2009.
[62] J. Kuhnhenn, S. K. Höffgen, and U. Weinand, "Quality assurance for irradiation tests of optical fibers: Uncertainty and reproducibility," *IEEE Trans. Nucl. Sci.*, vol. 56, no. 4, pp. 2160–2166, Aug. 2009.
[63] H. Henschel, S. K. Hoeffgen, J. Kuhnhenn, and U. Weinand, "High radiation sensitivity of Chiral Long period gratings," *IEEE Trans. Nucl. Sci.*, vol. 57, no. 5, pp. 2915–2922, Oct. 2010.
[64] N. Uesugi, T. Kuwabara, Y. Koyamada, Y. Ishida, and N. Uchida, "Optical loss increase of phosphor-doped silica fiber at high temperature in the long wavelength region," *Appl. Phys. Lett.*, vol. 43, pp. 327–329, 1983.
[65] G. G. Vienne, J. E. Caplen, L. Dong, J. D. Minelly, J. Nilsson, and D. N. Payne, "Fabrication and characterization of Yb^{3+}:Er^{3+} phosphosilicate fibers for lasers," *J. Lightw. Technol.*, vol. 16, pp. 1990–2001, 1998.
[66] E. M. Dianov, I. A. Bufetov, M. M. Bubnov, M. V. Grekov, S. A. Vasiliev, and O. I. Medvedkov, "Three-cascaded 1407-nm Raman laser based on phosphorus-doped silica fiber," *Opt. Lett.*, vol. 25, no. 6, pp. 402–404, 2000.
[67] D. L. Griscom, E. J. Friebele, K. J. Long, and J. W. Fleming, "Fundamental defect centers in glass: Electron spin resonance and optical absorption studies of irradiated phosphorus-doped silica glass and optical fibers," *J. Appl. Phys.*, vol. 54, pp. 3743–3743, 1983.
[68] J. Bisutti, S. Girard, and J. Baggio, "Radiation effects of 14 MeV neutrons on Ge- and P-doped optical fibres," *J. Non-Cryst. Solids*, vol. 353, pp. 461–465, 2007.
[69] J. Bisutti, S. Girard, C. Marcandella, and J. Baggio, "Infrared spectral dependencies of pulsed X-ray radiation-induced attenuation in single-mode optical fibers," presented at the 9th Eur. Conf. Radiation and its Effects on Components and Systems, Sep. 10–14, 2007, RADECS'2007.
[70] S. Girard, Y. Ouerdane, C. Marcandella, A. Boukenter, S. Quenard, and N. Authier, "Feasibility of radiation dosimetry with phosphorus-doped optical fibers in the ultraviolet and visible domain," *J. Non-Cryst. Solids*, vol. 357, pp. 1871–1874, 2011.
[71] H. Henschel, M. Körfer, J. Kuhnhenn, U. Weinand, and F. Wulf, "Fibre optic radiation sensor systems for particle accelerators," *Nucl. Instrum. Meth. Phys. Res. A*, vol. 526, no. 3, pp. 537–550, 2004.
[72] M. C. Paul, D. Bohra, A. Dhar, R. Sen, P. K. Bhatnagar, and K. Dasgupta, "Radiation response behavior of high phosphorous doped step-index multimode optical fibers under low dose gamma irradiation," *J. Non-Cryst. Solids*, vol. 355, no. 28–30, pp. 1496–1507, 2009.
[73] H. Henschel, O. Köhn, and H. U. Schmidt, "Optical fibres as radiation dosimeters," *Nucl. Instrum. Meth. Phys. Res. B*, vol. 69, pp. 307–314, 1992.
[74] S. Girard, Y. Ouerdane, A. Boukenter, C. Marcandella, J. Bisutti, J. Baggio, and J.-P. Meunier, "Integration of optical fibers in megajoule class laser environments: Advantages and limitations," *IEEE Trans. Nucl. Sci.*, to be published.
[75] E. M. Dianov, K. M. Golant, R. R. Khrapko, A. S. Kurkov, and A. L. Tomashuk, "Low-hydrogen silicon oxynitride optical fibers prepared by SPCVD," *J. Lightw. Technol.*, vol. 13, no. 7, pp. 1471–1474, 1995.
[76] A. L. Tomashuk, E. M. Dianov, K. M. Golant, R. R. Khrapko, and D. E. Spinov, "Performance of special radiation-hardened optical fibers intended for use in the telecom spectral windows at a megagray level," *IEEE Trans. Nucl. Sci.*, vol. 45, no. 3, pp. 1566–1569, Jun. 1998.
[77] S. Girard, J. Keurinck, A. Boukenter, J.-P. Meunier, Y. Ouerdane, B. Azaïs, P. Charre, and M. Vié, "γ-rays and pulsed X-ray radiation responses of nitrogen, germanium doped and pure silica core optical fibers," *Nucl. Instrum. Meth. Phys. Res. B*, vol. 215, no. 1–2, pp. 187–195, 2004.
[78] S. Girard, Y. Ouerdane, A. Boukenter, and J.-P. Meunier, "Transient radiation responses of silica-based optical fibers: Influence of modified chemical-vapor deposition process parameters," *J. Appl. Phys.*, vol. 99, no. 023104, 2006.
[79] A. L. Tomashuk and M. O. Zabezhailov, "Formation mechanisms of precursors of radiation-induced color centers during fabrication of silica optical fiber preform," *J. Appl. Phys.*, vol. 109, pp. 083103–083103, 2011.
[80] M. O. Zabezhailov, A. L. Tomashuk, I. V. Nikolin, and V. G. Plotnichenko, "Radiation-Induced absorption in high-purity silica fiber preforms," *Inorg. Mater.*, vol. 41, no. 3, pp. 315–321, 2005.
[81] B. Brichard, A. F. Fernandez, F. Berghmans, and M. Decréton, "Origin of the radiation-induced OH vibration band in polymer-coated optical fibers irradiated in a nuclear fission reactor," *IEEE Trans. Nucl. Sci.*, vol. 49, no. 6, pp. 2852–2856, Dec. 2002.
[82] K. Nagasawa, Y. Hoshi, Y. Ohki, and K. Yahagi, "Improvement of radiation resistance of pure silica core fibers by hydrogen treatment," *Jpn. J. Appl. Phys.*, vol. 24, pp. 1224–1228, 1985.
[83] O. Deparis, D. L. Griscom, P. Megret, M. Decreton, and A. Blondel, "Influence of the cladding thickness on the evolution of the NBOHC band in optical fibers exposed to gamma radiations," *J. Non-Cryst. Solids*, vol. 216, pp. 124–128, 1997.

[84] J. Kuhnehnn, H. Henschel, and U. Weinand, "Influence of coating material, cladding thickness, and core material on the radiation sensitivity of pure silica core step-index fibers," presented at the 8th Eur. Conf. Radiation and its Effects on Components and Systems (RADECS), 2005, paper A2.

[85] P. Borgermans, "Spectral and Kinetic Analysis of Radiation Induced Optical Attenuation in Silica: Towards Intrinsic Fiber Optic Dosimetry?," Thèse de doctorat, Vrije Universiteit, Brussels, 2001.

[86] O. Deparis, "Etude Physique Et Expérimentale De La Tenue Des Fibres Optiques Aux Radiations Ionisantes Par Spectrométrie Visible-Infrarouge," Ph.D. dissertation, Faculté Polytechnique de Mons, Mons, 1997.

[87] B. Brichard, "Systèmes à Fibres Optiques Pour Infrastructures Nucléaires: Du Durcissement Aux Radiations à l'application," Thèse de doctorat, IES—Institut d'Electronique du Sud, Montpellier, , 2008.

[88] S. Girard, "Analyse De La Réponse Des Fibres Optiques Soumises à Divers Environnements Radiatifs," Thèse de doctorat, Université de Saint-Etienne, Saint-Etienne, France, 2003.

[89] D. L. Griscom, M. E. Gingerich, and E. J. Friebele, "Model for the dose, dose-rate and temperature dependence of radiation-induced loss in optical fibers," *IEEE Trans. Nucl. Sci.*, vol. 41, no. 3, pp. 523–526, Jun. 1994.

[90] H. Henschel, O. Köhn, and H. U. Schmidt, "Influence of dose rate on radiation induced loss in optical fibres," in *Proc. SPIE Ser. 1399*, 1991, pp. 49–63.

[91] E. J. Friebele, C. G. Askins, and M. E. Gingerich, "Effect of low dose rate irradiation on doped silica core optical fibers," *Appl. Opt.*, vol. 23, no. 23, pp. 4202–4208, 1984.

[92] D. L. Griscom, "Fractal kinetics of radiation-induced point-defect formation and decay in amorphous insulators: Application to color centers in silica-based optical fibers," *Phys. Rev. B*, vol. 64, no. Doc. ID 174201, 2001.

[93] T. Wijnands, L. K. De Jonge, J. Kuhnhenn, S. K. Hoeffgen, and U. Weinand, "Optical absorption in commercial single mode optical fibers in a high energy physics radiation field," *IEEE Trans. Nucl. Sci.*, vol. 55, no. 4, pp. 2216–2222, Aug. 2008.

[94] T. Wijnands, K. Aikawa, J. Kuhnhenn, D. Ricci, and U. Weinand, "Radiation tolerant optical fibers: From sample testing to large series production," *J. Lightw. Technol.*, vol. 29, no. 22, pp. 3393–3400, 2011.

[95] O. Gilard, J. Thomas, L. Troussellier, M. Myara, P. Signoret, E. Burov, and M. Sotom, "Theoretical explanation of enhanced low dose rate sensitivity in erbium-doped optical fibers," *Appl. Opt.*, vol. 51, no. 13, pp. 2230–2235, 2012.

[96] A. T. Ramsey, W. Tighe, J. Bartolick, and P. D. Morgan, "Radiation effects on heated optical fibers," *Rev. Sci. Instrum.*, vol. 68, pp. 632–632, 1997.

[97] W. Tighe, P. Morgan, H. Adler, D. Cylinder, D. Griscom, D. Johnson, D. Palladino, and A. Ramsey, "Proposed experiment to investigate use of heated optical fibers for tokamak diagnostics during D-T discharges," *Rev. Sci. Instrum.*, vol. 66, pp. 907–907, 1995.

[98] M. León, P. Martín, D. Bravo, F. J. López, A. Ibarra, A. Rascón, and F. Mota, "Thermal stability of neutron irradiation effects on KU1 fused silica," *J. Nucl. Mater.*, vol. 374, pp. 386–389, 2008.

[99] P. Martín, M. León, A. Ibarra, and E. R. Hodgson, "Thermal stability of gamma irradiation induced defects for different fused silica," *J. Nucl. Mater.*, vol. 417, pp. 818–821, 2011.

[100] D. L. Griscom, "Nature of defects and defect generation in optical glasses," *Proc. SPIE*, vol. 541, pp. 38–59, 1985.

[101] D. L. Griscom, "On the natures of radiation-induced point defects in GeO_2-SiO_2 glasses: Reevaluation of a 26-year-old ESR and optical data set," *Opt. Mater. Exp.*, vol. 1, pp. 400–412, 2011.

[102] H. Henschel and O. Kohn, "Regeneration of irradiated optical fibres by photobleaching?," *IEEE Trans. Nucl. Sci.*, vol. 47, no. 3, pp. 699–704, Jun. 2000.

[103] K. Nagasawa, Y. Hoshi, Y. Ohki, and K. Yahagi, "Improvement of radiation resistance of pure silica core fibers by hydrogen treatment," *J. J. Appl. Phys.*, vol. 24, pp. 1224–1228, 1985.

[104] P. B. Lyons and L. D. Looney, "Enhanced radiation resistance of high-OH silica optical fibers," *Proc. SPIE*, vol. 1791, pp. 286–286, 1993.

[105] [Online]. Available: http://www.lle.rochester.edu/omega_facility/

[106] A. Johan, B. Azaïs, C. Malaval, G. Raboisson, and M. Roche, "ASTERIX, un nouveau moyen pour la simulation des effets de débit de dose sur l'électronique," *Ann. Phys.*, vol. 14, pp. 379–393, 1989.

[107] S. Girard, J. Baggio, and J. Bisutti, "14-MeV neutron, gamma-ray, and pulsed X-ray radiation-induced effects on multimode silica-based optical fibers," *IEEE Trans. Nucl. Sci.*, vol. 53, no. 6, pp. 3750–3757, Dec. 2006.

[108] S. Girard, J. Baggio, and M. Martinez, "Effect of high dose rate irradiations on COTS optical fibres," *Proc. SPIE*, vol. 5855, pp. 519–522, 2005.

[109] S. Girard, Y. Ouerdane, G. Origlio, C. Marcandella, A. Boukenter, N. Richard, J. Baggio, P. Paillet, M. Cannas, J. Bisutti, J.-P. Meunier, and R. Boscaino, "Radiation effects on silica-based preforms and Optical fibers-I: Experimental study with canonical samples," *IEEE Trans. Nucl. Sci.*, vol. 55, no. 6, pp. 3473–3482, Dec. 2008.

[110] S. Girard, C. Marcandella, A. Alessi, Y. Ouerdane, and A. Boukenter, "Transient radiation effects on opticalfibers for megajoule class lasers: Influence of MCVD process parameters," *IEEE Trans. Nucl. Sci.*, vol. 59, no. 6, pp. 2894–2901, Dec. 2012.

[111] E. K. Miller, G. S. Macrum, I. J. McKenna, H. W. Herrmann, J. M. Mack, C. S. Young, T. J. Sedillo, S. C. Evans, and C. J. Horsfield, "Accuracy of analog fiber-optic links for inertial confinement fusion diagnostics," *IEEE Trans. Nucl. Sci.*, vol. 54, no. 6, pp. 2457–2462, Dec. 2007.

[112] [Online]. Available: http://www.iter.org/

[113] P. Spuig, P. Defrasne, G. Martin, M. Moreau, P. Moreau, and F. Saint-Laurent, "An analog integrator for thousand second long pulses in Tore Supra," *Fusion Eng. Des.*, vol. 66–68, pp. 953–957, 2003.

[114] T. Yoshino, "Theory of the Faraday effect in optical fiber," *J. Opt. Soc. Amer.*, vol. 22, no. 9, Sep. 2005.

[115] P. Moreau, B. Brichard, A. Fil, P. Malard, P. Pastor, A. Le-Luyer, F. Samaille, and V. Massaut, "Test of fiber optic based current sensors on the Tore Supra Tokamak," *Fusion Eng. Des.*, vol. 86, pp. 1222–1226, 2011.

[116] G. Vayakis, L. Bertalot, P. Moreau, B. Brichard, A. Fil, P. Malard, P. Pastor, A. Le-Luyer, F. Samaille, and V. Massaut, "Test of fiber optic based current sensors on the Tore Supra Tokamak," *Fusion Eng. Des.*, vol. 86, pp. 1222–1226, 2011.

[117] A. Encheva, C. Walker, B. Brichard, M. S. Cheon, G. Chitarin, E. Hodgson, C. Ingesson, M. Ishikawa, T. Kondoh, H. Meister, P. Moreau, S. Peruzzo, S. Pak, G. Perez-Pichel, R. Reichle, D. Testa, M. Toussaint, L. Vermeeren, and V. Vershkov, "Nuclear technology aspects of ITER vessel-mounted diagnostics," *J. Nucl. Mater.*, vol. 417, pp. 780–786, 2011.

[118] B. Brichard, Development of Fiber Optic Current sensor for ITER 2010, Annual Progress Report, SCK CEN R-5050.

[119] M. Aerssens, A. Gusarov, B. Brichard, V. Massaut, P. Mégret, and M. Wuilpart, "Faraday effect based optical fiber current sensor for Tokamaks," presented at the ANIMMA-2011 Conf., Ghent, Belgium, 2011.

[120] S. P. Faile, J. J. Schmidt, and D. M. Roy, "Irradiation effects in glasses: Suppression by synthesis under high pressure hydrogen," *Science*, vol. 156, pp. 1593–1595, 1967.

[121] J. E. Shelby, "Radiation effects in hydrogen impregnated vitreous silica," *J. Appl. Phys.*, vol. 50, no. 5, pp. 3702–3706, 1979.

[122] K. Nagasawa, Y. Hoshi, Y. Ohki, and K. Yahagi, "Radiation effects on pure silica core optical fibers by gamma-rays: Relation between 2 eV band and non-bridging oxygen hole centers," *J. J. Appl. Phys.*, vol. 25, no. 3, pp. 464–468, 1986.

[123] B. Brichard, A. L. Tomashuk, H. Ooms, V. A. Bogatyrjov, S. N. Klyamkin, A. F. Fernandez, F. Berghmans, and M. Decréton, "Radiation assessment of hydrogen-loaded aluminium-coated pure silica core fibres for ITER plasma diagnostic applications," *Fusion Eng. Des.*, vol. 82, pp. 2451–2455, 2007.

[124] A. V. Bondarenko, A. P. Dyad'kin, Y. A. Kashchuk, A. V. Krasil'nikov, G. A. Polyakov, I. N. Rastyagaev, D. A. Skopintsev, S. N. Tugarinov, V. P. Yartsev, V. A. Bogatyrev, A. L. Tomashuk, S. N. Klyamkin, and S. E. Bender, "A study of radiation resistance of silica optical fibers under conditions of reactor irradiation," *Nucl. Instrum. Meth. Phys. Res. B*, vol. 49, no. 2, pp. 190–198, 2006.

[125] B. Brichard, S. Agnello, L. Nuccio, and L. Dusseau, "Comparison between point defect generation by gamma-rays in bulk and fibre samples of high purity amorphous SiO_2," *IEEE Trans. Nucl. Sci.*, vol. 55, no. 4, pp. 2121–2125, Aug. 2008.

[126] Y. Ikuta, K. Kajihara, M. Hirano, S. Kikugawa, and H. Hosono, "Effects of H_2 impregnation on excimer-laser-induced oxygen-deficient center formation in synthetic SiO_2 glass," *Appl. Phys. Lett.*, vol. 80, pp. 2917–3915, 2002.

[127] B. Amacker, CERN Main Optical Fibre Links [Online]. Available: http://ts-dep.web.cern.ch/ts-dep/groups/el/sections/OF/activities/Focern-monitoring%20Model%20(1).pdf, 2010-06-26

[128] M. N. Ott, "Radiation effects data on commercially available optical fiber: Database summary," presented at the Data Workshop NSREC, 2002, W5 paper.

[129] D. M. Scott, J. J. McAlarney, and R. A. Greenwell, "Induced attenuation and polarization hold properties in ECore fibers after Co-60 irradiation," in *Proc. SPIE Vol. 2290, Fiber Optic Materials and Components*, San Diego, CA, 1994, pp. 296–301.

[130] S. Girard, J. Keurinck, Y. Ouerdane, J.-P. Meunier, A. Boukenter, J.-L. Derep, B. Azaïs, P. Charre, and M. Vié, "Pulsed X-ray and rays irradiation effects on polarization-maintaining optical fibers," *IEEE Trans. Nucl. Sci.*, vol. 51, no. 5, pp. 2740–2746, Oct. 2004.

[131] E. J. Friebele, M. E. Gingerich, L. A. Brambani, C. C. Harrington, and S. J. Hickey, "Radiation effects in polarization maintaining fibers," in *Proc. SPIE Vol 1314, Fiber Optic'90*, 1990, pp. 146–154.

[132] R. Yamauchi, K. Himeno, T. Tsumanuma, and R. Dahlgren, "Specialty fibers for sensors and sensor components," in *Proc. SPIE Vol 2292, Fiber Optic and Laser Sensors XII*, 1994, pp. 328–338.

[133] M. J. Marrone, S. C. Rashleigh, E. J. Friebele, and K. J. Long, "Radiation- induced effects in a highly birefringent fiber," *Electron. Lett.*, vol. 20, no. 5, pp. 193–194, 1984.

[134] E. J. Friebele, L. A. Brambani, M. E. Gingerich, S. J. Hickey, and J. R. Onstott, "Radiation-induced attenuation in polarization maintaining fibers: Low dose rate response, stress, and materials effects," *Appl. Opt.*, vol. 28, no. 23, pp. 5138–5143, 1989.

[135] L. D. Looney and P. B. Lyons, "Transient radiation effects in polarization-maintaining fibers," in *Proc. SPIE 1791, Optical Materials Reliability and Testing: Benign and Adverse Environments*, paper 317.

[136] L. A. Brambani, E. J. Friebele, C. G. Askins, and M. E. Gingerich, "Radiation effects in polarization-maintaining optical fibers," presented at the Conf. Optical Fiber Communications, Washington, DC, 1988, paper TuG4.

[137] E. J. Friebele, K. J. Long, C. G. Askins, and M. E. Gingerich, "Overview of radiation effects in fiber optics," in *Proc. SPIE Vol 541, Radiation Effects in Optical Materials*, 1985, pp. 70–88.

[138] M. J. L. Valle, E. J. Friebele, F. V. Dimarcello, G. A. Miller, E. M. Monberg, L. R. Wasserman, P. W. Wisk, M. F. Yan, and E. M. Birtch, "Radiation-induced loss predictions for pure silica core, polarization-maintaining fibers," in *Proc. SPIE vol 6193*, 2006, pp. 61930J–61930J.

[139] Y. K. Chamorovskii, O. V. Butov, G. I. Ivanov, A. A. Kolosovskii, V. V. Voloshin, I. L. Vorob'ev, and K. M. Golant, "N-doped-silica-core polarization maintaining fibre for gyros and other sensors for application in space industry," in *Proc. SPIE Vol 7503*, 2009, pp. 75036T-1–75036T-1.

[140] E. W. Taylor, V. R. Wilson, M. L. Vigil, R. A. Lemire, and E. E. Thompson, "Ionization-induced nonequivalent absorption in a birefringent silica fiber," *IEEE Photon. Technol. Lett.*, vol. 1, pp. 248–249, 1989.

[141] G. M. Williams, M. A. Putnam, C. G. Askins, M. E. Gingerich, and E. J. Friebele, "Radiation effects in erbium-doped optical fibres," *Electron. Lett.*, vol. 28, no. 19, pp. 1816–1818, 1992.

[142] S. Girard, Y. Ouerdane, B. Tortech, C. Marcandella, T. Robin, B. Cadier, J. Baggio, P. Paillet, V. Ferlet-Cavrois, A. Boukenter, J.-P. Meunier, J. R. Schwank, M. R. Shaneyfelt, P. E. Dodd, and E. W. Blackmore, "Radiation effects on Ytterbium-and Ytterbium/Erbium-doped double-clad optical fibers," *IEEE Trans. Nucl. Sci.*, vol. 56, no. 6, pp. 3293–3299, Dec. 2009.

[143] B. P. Fox, K. Simmons-Potter, W. J. Thomes, and D. A. V. Kliner, "Gamma-radiation-induced photodarkening in unpumped optical fibers doped with rare-earth constituents," *IEEE Trans. Nucl. Sci.*, vol. 57, no. 3, pp. 1618–1625, Jun. 2010.

[144] S. Girard, B. Tortech, E. Regnier, M. Van Uffelen, A. Gusarov, Y. Ouerdane, J. Baggio, P. Paillet, V. Ferlet-Cavrois, A. Boukenter, J.-P. Meunier, F. Berghmans, J. R. Schwank, M. R. Shaneyfelt, J. A. Felix, E. W. Blackmore, and H. Thienpont, "Proton- and gamma-induced effects on erbium- doped optical fibers," *IEEE Trans. Nucl. Sci.*, vol. 54, no. 6, pp. 2426–2434, Dec. 2007.

[145] G. M. Williams and E. J. Friebele, "Space radiation effects on erbium-doped fiber devices: Sources, amplifiers, and passive measurements," *IEEE Trans. Nucl. Sci.*, vol. 45, no. 3, pp. 1531–1536, Jun. 1998.

[146] H. Henschel, O. Kohn, H. U. Schmidt, J. Kirchof, and S. Unger, "Radiation-induced loss of rare earth doped silica fibres," *IEEE Trans. Nucl. Sci.*, vol. 45, no. 3, pp. 1552–1557, Jun. 1998.

[147] M. Ott, Radiation effects expected for fiber laser/amplifier and rare-earth doped optical fibers, 2004, NASA GSFC, Parts, Packaging and Assembly Technologies Office Survey Report.

[148] A. Gusarov, M. Van Uffelen, M. Hotoleanu, H. Thienpont, and F. Berghmans, "Radiation sensitivity of EDFAs based on highly Er-doped fibers," *J. Lightw. Technol.*, vol. 27, no. 11, pp. 1540–1545, 2009.

[149] J. Ma, M. Li, L. Tan, Y. Zhou, S. Yu, and Q. Ran, "Experimental investigation of radiation effect on erbium-ytterbium co-doped fiber amplifier for space optical communication in low-dose radiation environment," *Opt. Exp.*, vol. 17, no. 18, pp. 15571–15577, 2009.

[150] T. S. Rose, D. Gunn, and G. C. Valley, "Gamma and proton radiation effects in erbium-doped fiber amplifiers: Active and passive measurements," *J. Lightw.Technol.*, vol. 19, no. 12, pp. 1918–1923, 2001.

[151] M. Li, J. Ma, L. Y. Tan, Y. P. Zhou, S. Y. Yu, J. J. Yu, and C. Che, "Investigation of the irradiation effect on erbium-doped fiber amplifiers composed by different density erbium-doped fibers," *Laser Phys.*, vol. 19, no. 1, pp. 138–142, 2009.

[152] P. Borgermans, B. Brichard, F. Berghmans, M. C. Decreton, K. M. Golant, A. L. Thomashuk, and I. V. Nikolin, "Dosimetry with optical fibers: Results for pure silica, phosphorous, and erbium doped samples," in *Proc. SPIE 4204*, 2001, vol. 151.

[153] B. Tortech, "Effets des radiations sur des fibres optiques dopées erbium," Thèse de doctorat, Université de Saint-Etienne, Saint-Etienne, France, 2008.

[154] K. V. Zotov, M. E. Likhachev, A. L. Tomashuk, M. L. Bubnov, M. V. Yashkov, A. N. Guryanov, and S. N. Klyamkin, "Radiation-resistant erbium-doped fiber for spacecraft applications," *IEEE Trans. Nucl. Sci.*, vol. 55, no. 4, pp. 2213–2215, Aug. 2008.

[155] M. Vivona, S. Girard, C. Marcandella, T. Robin, B. Cadier, M. Cannas, A. Boukenter, and Y. Ouerdane, "Influence of Cecodoping and H2 pre-loading on Er/Yb-doped fiber: Radiation response characterized by Confocal Micro-Luminescence," *J. Non-Cryst. Solids*, vol. 357, no. 8–9, pp. 1963–1965, 2011.

[156] K. V. Zotov, M. E. Likhachev, A. L. Tomashuk, A. F. Kosolapov, M. M. Bubnov, M. V. Yashkov, A. N. Guryanov, and E. M. Dianov, "Radiation resistant Er-doped fibers: Optimization of pump wavelength," *IEEE Photon. Technol. Lett.*, vol. 20, no. 17, pp. 1476–1478, 2008.

[157] S. Girard, M. Vivona, A. Laurent, B. Cadier, C. Marcandella, T. Robin, E. Pinsard, A. Boukenter, and Y. Ouerdane, "Radiation hardening techniques for Er/Yb doped optical fibers and amplifiers for space application," *Opt. Exp.*, vol. 20, pp. 8457–8465, 2012.

[158] Y. Sheng, L. Yang, H. Luan, Z. Liu, Y. Yu, and J. Li, "Improvement of radiation resistance by introducing CeO2 in Yb-doped silicate glasses," *J. Nucl. Mater.*, vol. 427, no. 1–3, pp. 58–61, 2012.

[159] M. Vivona, S. Girard, T. Robin, B. Cadier, L. Vaccaro, M. Cannas, A. Boukenter, and Y. Ouerdane, "Influence of Ce^{3+}Codoping on the photoluminescence excitation channels of phosphosilicate Yb/Er-doped glasses," *IEEE Photon. Technol. Lett.*, vol. 24, pp. 509–511, 2012.

[160] J. Thomas, M. Myara, L. Troussellier, E. Burov, A. Pastouret, D. Boivin, G. Mélin, O. Gilard, M. Sotom, and P. Signoret, "Radiation-resistant erbium-doped-nanoparticles optical fiber for space applications," *Opt. Express*, vol. 20, pp. 2435–2444, 2012.

[161] S. Girard, L. Mescia, M. Vivona, A. Laurent, Y. Ouerdane, C. Marcandella, F. Prudenzano, A. Boukenter, T. Robin, P. Paillet, V. Goiffon, B. Cadier, M. Cannas, and R. Boscaino, "Coupled experiment/simulation approach for the design of radiation-hardened rare-earth doped optical fibers and amplifiers," in *Proc. 12th Eur. Conf. Radiation and Its Effects on Components and Systems*, 2011, pp. 305–313, IEEE.

[162] M. Decréton, V. Massaut, and P. Borgermans, "Potential benefit of fibre optics in nuclear applications: The case of decomissioning and waste storage activities," in *Proc. SPIE Optical Fibre Sensing and Systems in Nuclear Environment*, Mol, Belgium, 1994, pp. 2–10.

[163] F. Jensen, E. Takada, M. Nakazawa, T. Kakuta, and S. Yamamoto, "Distributed Raman temperature measurement system for monitoring of nuclear power plant coolant loops," *Proc. Int. Soc. Optical Engineering (SPIE)*, vol. 2895, pp. 132–144, 1996.

[164] A. Kimura, E. Takada, K. Fujita, M. Nakazawa, H. Takahashi, and S. Ichige, "Application of a Raman distributed temperature sensor to the experimental fast reactor JOYO with correction techniques," *Meas. Sci. Technol.*, vol. 12, no. 7, pp. 966–973, 2001.

[165] F. Berghmans, F. Vos, and M. Decréton, "Evaluation of three different optical fibre temperature sensor types for application in gamma-radiation environment," *IEEE Trans. Nucl. Sci.*, vol. 45, pp. 1537–1542, 1998.

[166] A. F. Fernandez *et al.*, "Radiation-tolerant Raman distributed temperature monitoring system for large nuclear infrastructures," *IEEE Trans. Nucl. Sci.*, vol. 52, no. 6, pp. 2689–2694, Dec. 2005.

[167] D. Alasia *et al.*, "The effects of gamma-radiation on the properties of Brillouin scattering in standard Ge-doped optical fibres," *Meas. Sci. Technol.*, vol. 17, no. 5, pp. 1091–1094, 2006.
[168] X. Phéron, S. Girard, A. Boukenter, B. Brichard, S. Delepine-Lesoille, J. Bertrand, and Y. Ouerdane, "High γ-ray dose radiation effects on the performances of Brillouin scattering based optical fiber sensors," *Opt. Exp.*, vol. 20, pp. 26978–26985, 2012.
[169] H. Bueker, F. W. Haesing, and E. Gerhard, "Physical properties and concepts for applications of attenuation-based fiber optic dosimeters for medical instrumentation," *Proc. SPIE*, vol. 1648, pp. 63–70, 1992.
[170] B. Brichard, P. Borgermans, F. Berghmans, M. Decréton, A. L. Tomashuk, I. V. Nikolin, R. R. Khrapko, and K. M. Golant, "Dedicated optical fibres for dosimetry based on radiation-induced attenuation: Experimental results," in *Proc. SPIE*, 1999, vol. 3872, pp. 36–42.
[171] A. F. Fernandez, S. O'Keeffe, C. Fitzpatrick, B. Brichard, F. Berghmans, and E. Lewis, "Gamma dosimetry using commercial PMMA optical fibres for nuclear environments," in *Proc. SPIE*, 2005, vol. 5855, pp. 499–502.
[172] W. Gaebler, "Characteristics of fiber optic radiation detectors," *Proc. SPIE*, vol. 403, pp. 142–142, 1983.
[173] K. Imamura, T. Suzuki, T. Gozen, H. Tanaka, and S. Okamato, "Application of Nd^{3+} doped silica fibers to radiation sensing devices," *Proc. SPIE*, vol. 787, pp. 62–68, 1987.
[174] R. H. West *et al.*, "The use of optical-time domain reflectometers to measure radiation-induced losses in optical fibers," *J. Lightw. Technol.*, vol. 12, no. 4, pp. 614–620, 1994.
[175] H. Henschel *et al.*, "Radiation-induced loss of rare earth doped silica fibres," *IEEE Trans. Nucl. Sci.*, vol. 45, no. 3, pp. 1552–1557, Jun. 1998.
[176] H. Henschel *et al.*, "Fibre optic radiation sensor systems for particle accelerators," *Nucl. Instrum. Meth. Phys. Res. A*, vol. 526, no. 3, pp. 537–550, 2004.
[177] L. Dusseau and J. Gasiot, "Online and real time dosimetry using optically stimulated luminescence," *Int. J. High Speed Electron. Syst.*, vol. 14, pp. 605–623, 2004.
[178] A. L. Huston, B. L. Justus, P. L. Falkenstein, R. W. Miller, H. Ning, and R. Altemus, "Remote optical fiber dosimetry," *Nucl Instrum. Meth. Phys. Res. B*, vol. 184, pp. 55–67, 2001.
[179] B. Brichard *et al.*, "Fibre-optic gamma-flux monitoring in a fission reactor by means of Cerenkov radiation," *Meas. Sci. Technol.*, vol. 18, no. 10, pp. 3257–3257, 2007.
[180] P. Gouat *et al.*, "Present status of the Belgian contribution to the validation and design activities for the development of the IFMIF radiation-testing modules," *Fusion Eng. Des.*, vol. 86, no. 6–8, pp. 627–631, 2011.
[181] Characteristics of a Single Mode Optical Fibre and Cable, IUT-TG652 (2009-11).
[182] E. J. Friebele and D. L. Griscom, "Radiation effects in glass," in *Treatise on Materials Science and Technology*, M. T. Doremus, Ed. New York: Academic, 1979.
[183] R. A. B. Devine, "On the physical models of annealing of radiation induced defects in amorphous SiO_2," *Nucl Instrum. Meth. Phys. Res. B*, vol. 46, no. 1–4, pp. 261–264, 1990.
[184] D. T. H. Liu and A. R. Johnston, "Theory of radiation-induced absorption in optical fibers," *Opt. Lett.*, vol. 19, no. 8, pp. 548–550, 1994.
[185] M. Kyoto, Y. Chigusa, M. Ohe, H. Go, M. Watanabe, T. Matsubara, T. Yamamoto, and S. Okamoto, "Gamma-Ray radiation hardened properties of Pure silica core single-mode fiber and its data link system in radioactive environments," *J. Lightw. Technol.*, vol. 10, no. 3, pp. 289–294, 1992.
[186] O. Gilard, M. Caussanel, H. Duval, G. Quadri, and F. Reynaud, "New model for assessing dose, dose rate, and temperature sensitivity of radiation-induced absorption in glasses," *J. Appl. Phys.*, vol. 108, pp. 093115–093115, 2010.
[187] V. A. Mashkov, W. R. Austin, L. Zhang, and R. G. Leisure, "Fundamental role of creation and activation in radiation-induced defect production in high-purity amorphous SiO2," *Phys. Rev. Lett.*, vol. 76, pp. 2926–2929, 1996.
[188] P. W. Levy, "Overview of nuclear radiation damage processes phenomenological features of radiation damage in crystals and glasses," *Proc. SPIE*, vol. 541, pp. 2–24, 1985.
[189] H. Imai and H. Hirashima, "Intrinsic- and extrinsic-defect formation in silica glasses by radiation," *J. Non-Cryst. Solids*, vol. 179, pp. 202–213, 1994.
[190] P. Borgermans and B. Brichard, "Kinetic models and spectral dependencies of the radiation-induced attenuation in pure silica fibers," *IEEE Trans. Nucl. Sci.*, vol. 49, pp. 1439–1445, 2002.
[191] E. J. Friebele, M. E. Gingerich, and D. L. Griscom, "Survivability of optical fibers in space," in *Proc. SPIE*, 1992, vol. 1791, pp. 177–188.
[192] J. L. Bourgade, A. E. Costley, R. Reichle, E. R. Hodgson, W. Hsing, V. Glebov, M. Decreton, R. Leeper, J. L. Leray, M. Dentan, T. Hutter, A. Moroño, D. Eder, W. Shmayda, B. Brichard, J. Baggio, L. Bertalot, G. Vayakis, M. Moran, T. C. Sangster, L. Vermeeren, C. Stoeckl, S. Girard, and G. Pien, "Diagnostic components in harsh radiation environments: Possible overlap in R&D requirements of inertial confinement and magnetic fusion systems," *Rev. Sci. Instrum.*, vol. 79, pp. 10F304–10F304, 2008.
[193] S. Girard, N. Richard, Y. Ouerdane, G. Origlio, A. Boukenter, L. Martin-Samos, P. Paillet, J.-P. Meunier, J. Baggio, M. Cannas, and R. Boscaino, "Radiation effects on silica-based preforms and optical fibers-II: Coupling Ab initio Simulations and experiments," *IEEE Trans. Nucl. Sci.*, vol. 55, no. 6, pp. 3508–3514, Dec. 2008.
[194] N. Richard, S. Girard, L. Martin-Samos, V. Cuny, A. Boukenter, Y. Ouerdane, and J.-P. Meunier, "First principles study of oxygen-deficient centers in pure and Ge-doped silica," *J. Non-Cryst. Solids*, vol. 357, pp. 1994–1999, 2011.
[195] [Online]. Available: http://news.bull.com/bulldirect/2011/08/19/tera-100-once-again-crowned-as-europes-most-powerful-supercomputer/
[196] M. van Schilfgaarde, T. Kotani, and S. Faleev, "Quasiparticle self-consistent GW theory," *Phys. Rev. Lett.*, vol. 96, pp. 226402–226402, 2006.
[197] G. Onida, L. Reining, and A. Rubio, "Electronic excitations: Density-functional versus many-body Green's-function approaches," *Rev. Mod. Phys.*, vol. 74, pp. 601–601, 2002.
[198] L. Martin-Samos, N. Richard, S. Girard, A. Boukenter, Y. Ouerdane, and J.-P. Meunier, "First-principles study of electronic and optical properties of intrinsic defects in a-SiO2," *Phys. Rev. B*, 2012.
[199] P. V. Sushko, S. Mukhopadhyay, A. S. Mysovsky, V. B. Sulimov, A. Taga, and A. L. Shluger, "Structure and properties of defects in amorphous silica: New insights from embedded cluster calculations," *J. Phys.: Condens. Matter*, vol. 17, pp. S211–S211, 2005.
[200] A. V. Kimmel, P. V. Sushko, and A. L. Shluger, "Structure and spectroscopic properties of trapped holes in silica," *J. Non-Cryst. Solids*, vol. 353, pp. 599–604, 2007.
[201] G. Pacchioni and R. Ferrario, "Optical transitions and EPR properties of two-coordinated Si, Ge, Sn and related H(I), H(II), and H(III) centers in pure and doped silica from ab initio calculations," *Phys. Rev. B*, vol. 58, pp. 6090–6096, 1998.